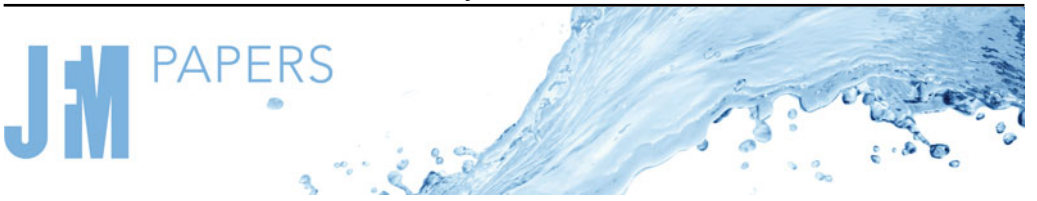
*J. Fluid Mech.* (2026), *vol.* 1040, A37, doi:10.1017/jfm.2026.11884




# Unsteady flow of a two-layer fluid generated by a moving circular cylinder

**Vasily K. Kostikov**[1], **Alexander E. Golikov**[2] **and Nikolay I. Makarenko**[2]

[1]Department of Applied Mathematics, School of Mathematics and Physics, Xi'an Jiaotong-Liverpool University, Suzhou 215123, PR China

[2]Lavrentyev Institute of Hydrodynamics, Novosibirsk 630090, Russia

**Corresponding author:** Vasily K. Kostikov, vasily.kostikov@xjtlu.edu.cn

(Received 19 November 2025 UTC; revised 11 June 2026 UTC; accepted 1 July 2026 UTC)

We consider the plane problem of unsteady flow generated on the interface of a two-layer infinite fluid by a smooth start of a horizontal circular cylinder. The problem is reduced to an integro-differential system of equations for the functions defining the normal and tangential velocity components of fluid particles on the interface and the shape of the interface. A small-time asymptotic solution is constructed for the cylinder moving with constant acceleration from the state of rest without intersecting the interface, whether moving below or above it. The disturbances created at the interface by unsteady motion of the cylinder are investigated for various density ratios and directions of motion. The influence of the density difference on the interface flow and the hydrodynamic forces acting on the cylinder is investigated. An analysis of the asymptotic solution, along with a comparison to free surface flow in a single-layer fluid, reveals that in a two-layered fluid with small density difference, the nonlinear effects and gravitational force contribute negligibly during the initial stage of the cylinder motion.

**Key words:** wave-structure interactions, general fluid mechanics

## 1. Introduction

The water in the ocean is naturally stratified due to density, salinity and temperature variations along the water depth. In the ocean, the significant increase in density, driven by changes in temperature and salinity, may be confined within a thin transient region called the pycnocline, above and below which the fluid density is practically constant. The density stratification is observed in fjords and harbours, where the water column consists of a layer of relatively fresh and less dense water (due to the input from rivers and glaciers) overlying a deep body of saltier and denser water. In muddy coastal regions, the boundary between the clear water and the cohesive sediment at the bottom is quite sharp. Therefore, a two-layer fluid model can be regarded as a viable approximation of real marine conditions.

© The Author(s), 2026. Published by Cambridge University Press.



https://doi.org/10.1017/jfm.2026.11884 Published online by Cambridge University Press

The problem of internal waves in the presence of an obstacle arises in connection with the modelling of an underwater pipe bridge or a self-propelled autonomous underwater vehicle, because the fluid stratification can induce significant effects on these underwater structures (Nansen 1897; Ekman 1904; Miloh *et al.* 1993; Parau *et al.* 2007; Grue *et al.* 2016). From a physical viewpoint, a circular cylinder is a reasonable model for such underwater structures. Hence, it is of practical importance to understand the interaction mechanism between a circular cylinder and a thin interface separating lighter and heavier fluids of uniform density.

The interaction of waves with a horizontal circular cylinder in a single-layered fluid is a problem of fundamental interest with applications in marine hydrodynamics. The diffraction and radiation problems within a linear formulation were solved theoretically by Havelock (1927), Dean (1948), Ursell (1950), Grue & Palm (1985), among others. In these classical studies, a submerged body was approximated by a suitable distribution of singularities and the solution was obtained at a great distance from the body. The contribution of nonlinear terms in the free surface boundary conditions was addressed by Tuck (1965), who developed a method based on the Wehausen scheme to calculate higher-order pressure terms. Ogilvie (1963) extended the results of Dean (1948) and Ursell (1950) to the nonlinear case, and analytically calculated the second-order forces acting on the cylinder using a perturbation technique. Dagan & Miloh (1982) considered higher-order free surface effects for a cylinder in oscillatory motion by employing a perturbation expansion in the amplitude of the oscillatory singularity.

To date, the amount of theoretical research on nonlinear wave–structure interaction problems has diminished with the development of more efficient numerical simulation tools, capable of handling complex geometries and nonlinear free surface boundary conditions (see, e.g. Haussling & Coleman 1979; Telste 1987; Moyo & Greenhow 2000). Despite their great success, numerical models are computationally expensive and often fail to provide accurate predictions for the transient regime resulting from the impulsive start or acceleration of a body. Tyvand & Miloh (1995) proposed investigating the short-time evolution of wave motion produced by a cylinder starting to move impulsively at a constant speed by using a small-time expansion in an auxiliary plane of bi-polar coordinates. Later, Tyvand & Kostikov (2023) generalised this work by accounting for the interaction between simultaneous impulsive velocity and impulsive acceleration. Makarenko (2003) obtained the same small-time asymptotic solution for a cylinder of small radius by using the boundary equations method. Kostikov & Makarenko (2018) extended this solution by incorporating higher-order nonlinear effects up to the fourth-order with respect to the radius of the cylinder. This approach, in particular, made it possible to describe splash-jet formation and small-scale riding waves over a submerging cylinder. In their investigation of the inertial exit dynamics of a horizontal circular cylinder, Vincent *et al.* (2026) pointed out that the simplified models of Tyvand & Miloh (1995) and Kostikov & Makarenko (2018) have the intrinsic shortcoming of predicting non-physical and exaggerated free surface behaviour outside their range of applicability. In search of a more accurate asymptotic solution, Pardo & Nedic (2021) implemented a recursive scheme based on the method of Makarenko (2003) and numerically calculated terms up to the eighth order in the asymptotic time expansion. This semi-analytical approach has a wider temporal range and overcomes the limitations of a small cylinder size. Golikov & Makarenko (2024) revisited the problem from the perspective of a freely moving cylinder and calculated the hydrodynamic forces (Golikov & Makarenko 2022). Semenov *et al.* (2021) reduced the problem of the impulsive impact of a cylindrical body of arbitrary cross-section in a container with a free surface to a system of boundary integral equations using the integral hodograph method and solved the resulting equations numerically.



https://doi.org/10.1017/jfm.2026.11884 Published online by Cambridge University Press

A comparatively small amount of research is dedicated to the problem of body motion in a stratified fluid, even within a linear approximation. Stokes (1847) and Rayleigh (1882) were the first to study the propagation of interfacial waves in an unbounded two-layer fluid without an obstacle. The development of theoretical models for wave–structure interaction in a two-layered fluid began relatively recently and was initially concerned mainly with steady flows or diffraction problems. Bukreev *et al.* (1983) performed a theoretical and experimental study of waves generated on the interface by the unsteady translational motion of a submerged circular cylinder in a horizontal direction. In their linear formulation, the body was replaced by a dipole with a variable moment. Linton & McIver (1995) used linear water wave theory to consider the interaction of waves with a horizontal cylinder in a fluid consisting of a layer of finite depth bounded above by a free surface and below by an infinite layer of fluid of greater density. They described the wave scattering problem using Green's theorem and a multipole expansion technique originally developed by Ursell (1950) for a non-stratified fluid, which was later adapted by Kassem (1982) for a two-layer fluid bounded above and below by rigid walls. Khabakhpasheva & Sturova (1998) derived the solution to the linear problem of a uniform horizontal flow of a two-layer fluid of infinite depth past a circular cylinder. They conformally mapped the physical plane of the flow onto the region between two concentric circles and represented the potentials in the form of an infinite series of fundamental solutions of the Laplace equation. Das & Mandal (2007) investigated wave scattering by a horizontal circular cylinder in a two-layer fluid covered by an ice sheet using the method of multipole expansion. Penetration of a body through the interface of a two-layer fluid has been investigated theoretically by Motygin & Kuznetsov (2011), who proposed supplementary boundary conditions for the linear problem of water waves in the presence of an interface-crossing cylinder. The laboratory experiments of Pierson & Magnaudet (2018*a*,*b*) involving a sphere moving through the interface of two superposed viscous fluids are worth mentioning in this regard.

The unsteady nonlinear hydrodynamic forces acting on a horizontal circular cylinder moving in a two-layer fluid and the resulting deformations of the interface are of considerable practical importance and theoretical interest. Havelock (1949) established the mathematical framework, using linear wave theory, for calculating the wave resistance on a submerged cylinder moving at constant speed in a single-layer fluid. However, experimental and theoretical investigations into the evolution of forces acting on an accelerating object in a two-layer fluid remain challenging. This inherent difficulty explains why recent studies on internal waves have focused on the diffraction problem, analysing the scattering characteristics of submerged or floating objects and accounting for periodic steady-state wave loads (Ogilvie 1963; Grue & Palm 1985). Experimental tests on the interaction of internal waves with a submerged cylinder under stratified conditions are rare (see Ermanyuk & Gavrilov 2005). In many studies, the object's motion is driven by buoyancy and few studies have analysed the characteristics of interfacial waves through the controlled motion of an obstacles (Seong *et al.* 2024; Kim *et al.* 2025). Existing data on hydrodynamic forces acting on a body moving in proximity to a fluid interface were obtained primarily from single-fluid studies, including investigations into the water exit problem (Telste 1987; Moyo & Greenhow 2000; Vincent *et al.* 2026) and the motion of a cylinder accelerating to a constant horizontal speed (Haussling & Coleman 1979). Previous work on wave resistance in stratified fluids includes the study by Motygin & Kuznetsov (1997) on the forward motion of a cylinder in a two-layer fluid under a linear formulation, for which asymptotic formulae were derived. To the best of our knowledge, the most recent study of the unsteady problem of a contour approaching an interface between two liquid media was presented by Gorlov (2000). Hence, the aim



https://doi.org/10.1017/jfm.2026.11884 Published online by Cambridge University Press

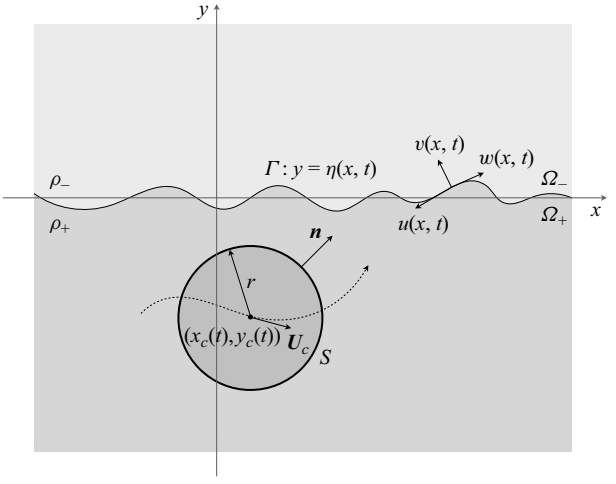



Figure 1. Scheme of motion of a cylinder in the lower layer of a two-layer fluid.

of the present work is to provide a higher-order asymptotic solution for the early stage of the flow when a cylinder starts to move in proximity to the interface of a two-layered fluid and to elucidate the main physical processes at play. This paper applies the method of reduction to boundary integro-differential equations (Makarenko 2003) and presents a systematic extension of the small-time asymptotic solution, originally obtained by Kostikov & Makarenko (2018) for free surface flow generated by a moving underwater obstacle, to the two-fluid case.

The rest of the paper is structured as follows. Section 2 presents the problem statement for the flow of a two-layer fluid in the presence of an obstacle. Section 3 transforms the governing equations into a closed evolution system of integro-differential equations defined on the interface dividing the two fluid layers. In § 4, a recurrent chain of equations derived from a small-time expansion is solved to obtain an approximate solution in the form of a power series, the coefficients of which are rational functions of the spatial variable. Section 5 details the calculation of hydrodynamic forces acting on the cylinder. Section 6 compares the obtained analytical solution with the results from linear wave theory. In § 7, the role of the two-layer fluid configuration and the effect of density stratification on the dynamics of the interfacial flow are comprehensively analysed. The paper closes with the main observations and conclusions in § 8. Appendices A and B contain auxiliary information related to the derivation of the asymptotic solution in §§ 4 and 5.

## 2. Formulation of the problem

The flow domain consists of two semi-infinite regions, $\Omega_+$ and $\Omega_-$, occupied by fluids of densities $\rho_+$ and $\rho_-$ ($\rho_+ > \rho_-$), respectively. These regions are connected through the interface $\Gamma : y = \eta(x, t)$, whose equilibrium position is at $y = 0$, as shown in figure 1. A circular cylinder of radius $r$ starts moving in one of the layers without intersecting the interface, following the prescribed trajectory $(x_c(t), y_c(t))$ for $t > 0$.

In subsequent derivations and discussion, we will use non-dimensional variables. The density of the lower layer $\rho_+$, the initial submergence depth $h$ and the characteristic speed of the cylinder $u_0$ form a dimensionally independent set. Consequently, the quantities $h/u_0$ and $\rho u_0^2$ determine the units of time and pressure, respectively. The non-dimensional density of the upper layer, which characterises the density ratio of the two fluids, is denoted



https://doi.org/10.1017/jfm.2026.11884 Published online by Cambridge University Press

by $\rho = \rho_-/\rho_+$. By definition, $0 \leqslant \rho < 1$. For subsequent discussion, it will be useful to introduce the Atwood number, which characterises the density difference of the two layers:

$$a = \frac{\rho_+ - \rho_-}{\rho_+ + \rho_-} = \frac{1-\rho}{1+\rho}. \tag{2.1}$$

In the special case, when $a = 1$, we deal with the free surface flow of a one-layer fluid. The limiting case of $a = 0$, when a two-layer fluid becomes homogeneous and the interface disappears, has no meaning in the current formulation.

The fluid velocity vector $\boldsymbol{U}_\pm = (U_\pm, V_\pm)$ and pressure $p_\pm$ in both layers should satisfy the irrotational Euler equations

$$\frac{\partial U_\pm}{\partial x} + \frac{\partial V_\pm}{\partial y} = 0, \quad \frac{\partial U_\pm}{\partial y} - \frac{\partial V_\pm}{\partial x} = 0, \quad (x, y) \in \Omega_\pm, \tag{2.2}$$

$$\frac{\partial U_\pm}{\partial t} + U_\pm \frac{\partial U_\pm}{\partial x} + V_\pm \frac{\partial U_\pm}{\partial y} + \frac{1}{\rho_*}\frac{\partial p_\pm}{\partial x} = 0, \quad (x, y) \in \Omega_\pm, \tag{2.3}$$

$$\frac{\partial V_\pm}{\partial t} + U_\pm \frac{\partial V_\pm}{\partial x} + V_\pm \frac{\partial V_\pm}{\partial y} + \frac{1}{\rho_*}\frac{\partial p_\pm}{\partial y} = -\lambda, \quad (x, y) \in \Omega_\pm. \tag{2.4}$$

Here, the non-dimensional density parameter $\rho_*$ is equal to $\rho$ in the upper layer and to unity in the lower layer. The important physical parameter $\lambda = gh/u_0^2$, defined with the gravity acceleration $g$, is the square of the inverse Froude number. The fully nonlinear kinematic and dynamic boundary conditions at the interface $\Gamma(t) : y = \eta(x, t)$ are

$$\frac{\partial \eta}{\partial t} + U_\pm \frac{\partial \eta}{\partial x} = V_\pm, \quad (x, y) \in \Gamma, \tag{2.5}$$

$$p_+ = p_-, \quad (x, y) \in \Gamma. \tag{2.6}$$

The boundary condition on the moving cylinder situated in the lower layer takes the form

$$(\boldsymbol{U}_+ - \boldsymbol{U}_c) \cdot \boldsymbol{n} = 0, \quad (x, y) \in S, \tag{2.7}$$

where the vector $\boldsymbol{n}$ is the unit normal to the surface of the cylinder and the vector $\boldsymbol{U}_c(t) = (\dot{x}_c(t), \dot{y}_c(t))$ is the prescribed non-dimensional velocity of the cylinder. In the case of a cylinder in the upper layer, the subscript $_+$ in (2.7) must be changed to $_-$. We assume that both fluids are at rest at infinity, as described by the condition

$$\eta \to 0, \quad \boldsymbol{U}_\pm \to 0, \quad |\boldsymbol{x}| \to \infty. \tag{2.8}$$

At the initial time $t = 0$, the cylinder centre is placed at the point $(x_c(0), y_c(0) = (0, \pm 1)$, where plus and minus signs correspond to the cylinder location in the lower and upper layer, respectively. The initial velocity field $\boldsymbol{U}_\pm(0) = (U_\pm(0), V_\pm(0))$ must satisfy the compatibility conditions

$$\frac{\partial U_\pm}{\partial x} + \frac{\partial V_\pm}{\partial y} = 0, \quad \frac{\partial U_\pm}{\partial y} - \frac{\partial V_\pm}{\partial x} = 0, \quad (x, y) \in \Omega_\pm, \tag{2.9}$$

$$(\boldsymbol{U}_\pm(0) - \boldsymbol{U}_c(0)) \cdot \boldsymbol{n} = 0, \quad (x, y) \in S. \tag{2.10}$$

The initial data determine velocity circulation around the contour of the cylinder as

$$\gamma = \oint_S U_\pm(0)\,\mathrm{d}x + V_\pm(0)\,\mathrm{d}y, \tag{2.11}$$

which remains constant at $t > 0$ due to the Kelvin theorem. Here, the index $+$ or $-$ is chosen, depending on the location of the cylinder below or above the interface, respectively. The non-zero velocity $U_\pm(0)$ at the initial time corresponds to the problem



https://doi.org/10.1017/jfm.2026.11884 Published online by Cambridge University Press

of an impulsive start of the body starting to move with non-zero speed. In this study, however, we consider the smooth start of the cylinder with constant acceleration from rest, corresponding to the initial data $\boldsymbol{U}_{\pm}(0) = (0, 0)$ and $\boldsymbol{U}_c(0) = (0, 0)$, for which the compatibility conditions are automatically satisfied.

## 3. Reduction to the boundary

A challenging aspect of water wave problems in a nonlinear formulation is that the boundary conditions are enforced on an unknown boundary, the position of which is part of the solution. The mathematical problem considered here allows for a closed formulation in the form of a system of integro-differential equations valid on the moving boundary $\Gamma(t) : y = \eta(x, t)$. The tangential and normal fluid velocities on the interface in both layers are determined as projections of the fluid-particle velocity vector $\boldsymbol{U}_{\pm} = (U_{\pm}, V_{\pm})$ onto the tangent $(1, \eta_x)$ and normal $(-\eta_x, 1)$ vectors at the corresponding point on the interface $y = \eta(x, t)$:

$$u_{\pm} = U_{\pm} + \eta_x V_{\pm}, \quad v_{\pm} = V_{\pm} - \eta_x U_{\pm}, \quad y = \eta(x, t). \tag{3.1}$$

We assume that two fluids do not mix and therefore the components of fluid-particle velocities in two layers normal to the interface $y = \eta(x, t)$ must be equal: $v_+ = v_-$. To minimise the use of subscripts, we adopt the notation $u = u_+$, $w = u_-$, $v = v_+ = v_-$.

In the new variables, the kinematic boundary condition (2.5) reduces to a single equation

$$\eta_t = v. \tag{3.2}$$

Projecting the momentum equations (2.3) and (2.4) in both fluids onto the tangent line to the interface $\boldsymbol{\tau} = (1, \eta_x)$, and using the dynamic boundary condition (2.6) allow us to exclude fluid pressure $p_{\pm}$ from the problem formulation:

$$u_t - \rho w_t + \frac{1}{2}\frac{\partial}{\partial x}\left(\frac{u^2 - \rho w^2 - 2\eta_x v(u - \rho w) - (1 - \rho)v^2}{1 + \eta_x^2}\right) + (1 - \rho)\lambda\eta_x = 0. \tag{3.3}$$

According to the method developed by Ovsyannikov *et al.* (1985), differential equations (3.2) and (3.3) must be complemented by two boundary integral equations following from the Cauchy integral formula for the complex velocity function $F_{\pm}(z) = U_{\pm} - iV_{\pm}$, which is analytic in $\Omega_{\pm}$. The analyticity follows from (2.2), equivalent to the Cauchy–Riemann conditions for the velocity components $U_{\pm}$ and $V_{\pm}$. When the cylinder is located in the lower layer, the boundary integral equation for the lower layer $\Omega_+$ has the form

$$2\pi i F_+(z, t) = \int_{\Gamma(t)} \frac{F_+(\zeta, t)\mathrm{d}\zeta}{\zeta - z} + \frac{r^2}{(z - z_c(t))^2}\overline{\int_{\Gamma(t)} \frac{F_+(\zeta, t)\mathrm{d}\zeta}{\zeta - z_*(t)}} + \frac{\gamma}{z - z_c(t)} + \frac{2\pi i r^2 \dot{z}_c(t)}{(z - z_c(t))^2}, \tag{3.4}$$

where $z_*(t) = z_c(t) + r^2/\overline{z - z_c}$ is the inverse image of the complex point $z$ with respect to the circle centred at the point $z_c(t) = x_c(t) + iy_c(t)$. The constant $\gamma$ is the velocity circulation around the cylinder, as defined by (2.11). The boundary integral equation (3.4), which contains integrals over the free boundary $\Gamma(t)$ only, was first derived by Ovsyannikov *et al.* (1985) using the Cauchy integral formula for the analytic function $F_+(z, t)$ and the Milne–Thomson circle theorem. The derivation of this integral equation has been reproduced multiple times by Makarenko (2003), Kostikov & Makarenko (2018) and Pardo & Nedic (2021). A combination of real and imaginary parts of (3.4), evaluated at the interface, gives the real-valued version of the boundary integral equation. This can be written in operator form as follows:



https://doi.org/10.1017/jfm.2026.11884 Published online by Cambridge University Press

$$[I + A(\eta) + r^2 A^r(\eta)]v - [B(\eta) + r^2 B^r(\eta)]u = v^d. \tag{3.5}$$

Here, the integral operators $A$ and $B$ correspond to the problem of waves on the interface without a cylinder:

$$A(\eta)v(x) = \frac{1}{\pi} \int\!\!\!\!\!\!-_{-\infty}^{\infty} \frac{\eta(x) - \eta(s) - (x-s)\eta'(x)}{(x-s)^2 + [\eta(x) - \eta(s)]^2} v(s)\mathrm{d}s, \tag{3.6}$$

$$B(\eta)u(x) = \frac{1}{\pi} \int\!\!\!\!\!\!-_{-\infty}^{\infty} \frac{x - s + [\eta(x) - \eta(s)]\eta'(x)}{(x-s)^2 + [\eta(x) - \eta(s)]^2} u(s)\mathrm{d}s, \tag{3.7}$$

and the integral operators with superscripts $A^r$ and $B^r$ are responsible for interaction of the cylinder with the interface:

$$A^r(\eta)v(x) = \frac{1}{\pi} \int\!\!\!\!\!\!-_{-\infty}^{\infty} \frac{\left[\eta(s) - y_c - r^2 P(x)\right] Q'(x) - \left[s - x_c - r^2 Q(x)\right] P'(x)}{\left[\eta(s) - y_c - r^2 P(x)\right]^2 + \left[s - x_c - r^2 Q(x)\right]^2} v(s)\mathrm{d}s, \tag{3.8}$$

$$B^r(\eta)u(x) = \frac{1}{\pi} \int\!\!\!\!\!\!-_{-\infty}^{\infty} \frac{\left[\eta(s) - y_c - r^2 P(x)\right] P'(x) + \left[s - x_c - r^2 Q(x)\right] Q'(x)}{\left[\eta(s) - y_c - r^2 P(x)\right]^2 + \left[s - x_c - r^2 Q(x)\right]^2} u(s)\,\mathrm{d}s. \tag{3.9}$$

It should be noted that the above-mentioned dashed integrals are to be considered in the sense of the Cauchy principal value to account for the discontinuities of the kernel functions. Here, the functions $P(x)$ and $Q(x)$ are the generalised versions of the Poisson kernels:

$$P(x) = \frac{\eta(x) - y_c}{(x - x_c)^2 + (\eta(x) - y_c)^2}, \quad Q(x) = \frac{x - x_c}{(x - x_c)^2 + (\eta(x) - y_c)^2}, \tag{3.10}$$

which depend on the interface shape $\eta(x, t)$ and the coordinates of the cylinder $(x_c(t), y_c(t))$. The term $v^d$ is the normal component of the fluid velocity induced at the interface by a dipole of unit strength:

$$v^d(x) = 2r^2 \left(\dot{y}_c Q'(x) - \dot{x}_c P'(x)\right). \tag{3.11}$$

Here and in what follows, a prime denotes the derivative of an ordinary function with respect to the spatial coordinate $x$ and an upper dot signifies the derivative of a one-variable function with respect to the time variable $t$.

The analogue of the integral equation for the upper layer without a body can be obtained from (3.5) by omitting the terms $A^r v$, $B^r u$ and $v^d$, which are responsible for the interaction of the cylinder with the interface, and by inversing the signs preceding the integrals due to the reversed direction of integration:

$$[I - A(\eta)]v + B(\eta)w = 0. \tag{3.12}$$

The system of equations (3.2), (3.3), (3.5) and (3.12) forms a complete set of equations for the unknown interface $\eta$, the normal velocity $v$, and the tangential velocities $u$ and $w$ on the interface. This system fully defines the problem of interface waves generated by the arbitrary motion of a cylinder in the lower layer.

When the cylinder moves in the upper layer, the differential equations (3.2) and (3.3) on the interface remain the same, as they carry no information about the obstacle. However,



https://doi.org/10.1017/jfm.2026.11884 Published online by Cambridge University Press

the integral equations (3.5) and (3.12) exchange their roles due to the changed position of the cylinder relative to the interface. Consequently, the following integral equations must be satisfied on the interface:

$$\left[I - A(\eta) - r^2 A^r(\eta)\right] v + \left[B(\eta) + r^2 B^r(\eta)\right] w = v^d, \tag{3.13}$$

$$[I + A(\eta)]v - B(\eta)u = 0. \tag{3.14}$$

Equations (3.13) and (3.14) can be obtained from (3.5) and (3.12) by interchanging the functions $u$ and $w$, and inverting the signs of the integral operators. The dependence on time is omitted in the above-mentioned formulae, as it appears only as a parameter. In the next section, we will consider a cylinder moving in the lower layer below the interface for clarity of mathematical expressions, keeping in mind that the case of a cylinder in the upper layer can be treated similarly.

## 4. Small-time asymptotic solution

The boundary integro-differential equations (3.2), (3.3), (3.5) and (3.12) form a nonlinear evolution system, which is difficult to solve analytically. The integral operators in (3.5) and (3.12), while acting linearly on the unknown functions $u$, $w$ and $v$, have kernels that depend nonlinearly on the interface displacement $\eta$. This system can be solved for the initial stage of motion using a recursive scheme derived by expanding the involved variables into small-time series.

We consider the unsteady flow at the interface, induced by the smooth start of the cylinder, which is characterised by zero initial conditions:

$$u(x, 0) = w(x, 0) = v(x, 0) = \eta(x, 0) = 0. \tag{4.1}$$

The trajectory of the cylinder, moving in the lower layer of a two-layered fluid with constant acceleration from rest at an angle $\theta$ with respect to the horizontal axis, is defined by

$$(x_c(t),\, y_c(t)) = \left(t^2 \cos\theta,\, -1 + t^2 \sin\theta\right). \tag{4.2}$$

Kinematic boundary condition (3.2) and zero initial conditions (4.1) dictate the following structure of the power series of unknown functions with respect to the time variable $t$:

$$\eta(x, t) = t^2\eta_2(x) + t^3\eta_3(x) + \cdots, \qquad u(x, t) = tu_1(x) + t^2u_2(x) + \cdots, \tag{4.3}$$

$$w(x, t) = tw_1(x) + t^2w_2(x) + \cdots, \qquad v(x, t) = tv_1(x) + t^2v_2(x) + \cdots. \tag{4.4}$$

Substituting series (4.3)–(4.4) into (3.2)–(3.3) and grouping the terms of equal order, we obtain the following set of recursive relations between terms:

$$\eta_{n+1}(x) = \frac{1}{n+1} v_n(x), \tag{4.5}$$

$$u_n(x) - \rho w_n(x) = \phi_n(x), \tag{4.6}$$

where function

$$\phi_n(x) = -\frac{1}{2n}\frac{\partial}{\partial x}\left[\sum_{j=1}^{n-1}(u_j u_{n-j-1} - \rho w_j w_{n-j-1}) - 2\sum_{j+k+l=0}^{n-2}\eta_j(u_k - \rho w_k)v_l - (1-\rho)\sum_{j=1}^{n-1} v_j v_{n-j-1} + 2(1-\rho)\lambda\eta_{n-1}\right], \tag{4.7}$$



https://doi.org/10.1017/jfm.2026.11884 Published online by Cambridge University Press

inherits the structure of linear and nonlinear terms from boundary differential equation (3.3).

The leading-order terms in the time expansions of the generalised Poisson kernels $P(x)$ and $Q(x)$, defined by (3.10), can be found explicitly as

$$P(\eta) = p(x) + \Big[-p'(x)\cos\theta + q'(x)\sin\theta - q'(x)\eta_2(x)\Big]t^2 + \cdots, \tag{4.8}$$

$$Q(\eta) = q(x) + \Big[-p'(x)\sin\theta - q'(x)\cos\theta + p'(x)\eta_2(x)\Big]t^2 + \cdots. \tag{4.9}$$

The pair of functions

$$p(x) = \frac{1}{1+x^2}, \quad q(x) = \frac{x}{1+x^2} \tag{4.10}$$

forms a conjugate pair with respect to the Hilbert transform, which is defined by the convolution with Cauchy's kernel as

$$Hu(x) = \frac{1}{\pi} \int\!\!\!\!\!\!- \limits_{-\infty}^{\infty} \frac{u(s)}{x-s}\mathrm{d}s, \tag{4.11}$$

meaning that $Hp(x) = q(x)$ and $Hq(x) = -p(x)$. The functions $p(x)$ and $q(x)$, referred to here as Poisson kernels, will play a crucial role in constructing the solution to the problem. These functions decay at infinity and, thus, the Hilbert transform (4.11) is well-defined for them. The property of the Hilbert transform, that it coincides with its inverse up to a sign ($-H = H^{-1}$), will be used extensively in our study.

The time series for the integral operators, defined by (3.6)–(3.9), have the form

$$A(\eta) = t^2 A_2 + t^3 A_3 + \cdots, \quad B(\eta) = B_0 + t^4 B_4 + \cdots, \tag{4.12}$$

$$A^r(\eta) = A_0^r + t^2 A_2^r + \cdots, \quad B^r(\eta) = B_0^r + t^2 B_2^r + \cdots, \tag{4.13}$$

where the missing terms are accounted for by the form of the expansion (4.3) for $\eta$ and the smooth acceleration of the cylinder with zero initial speed. The coefficients of the leading-order in expansions (4.12)–(4.13), expressed via the integrals

$$A_2 v(x) = \frac{1}{\pi} \int\!\!\!\!\!\!- \limits_{-\infty}^{\infty} \frac{\eta_2(x) - \eta_2(s)}{(x-s)^2} v(s)\,\mathrm{d}s - \frac{1}{\pi}\eta_2'(x) \int\!\!\!\!\!\!- \limits_{-\infty}^{\infty} \frac{v(s)}{x-s}\mathrm{d}s, \tag{4.14}$$

$$B_0 u(x) = Hu(x), \tag{4.15}$$

$$A_0^r v(x) = \frac{1}{\pi} \int\!\!\!\!\!\!- \limits_{-\infty}^{\infty} \frac{\big(1-r^2p(x)\big)\,q'(x) - \big(s-r^2q(x)\big)\,p'(x)}{\big(1-r^2p(x)\big)^2 + \big(s-r^2q(x)\big)^2} v(s)\mathrm{d}s, \tag{4.16}$$

$$B_0^r u(x) = \frac{1}{\pi} \int\!\!\!\!\!\!- \limits_{-\infty}^{\infty} \frac{\big(1-r^2p(x)\big)\,p'(x) + \big(s-r^2q(x)\big)\,q'(x)}{\big(1-r^2p(x)\big)^2 + \big(s-r^2q(x)\big)^2} u(s)\,\mathrm{d}s \tag{4.17}$$

are the crucial integral components, contributing to the small-time asymptotic solution.

The normal fluid velocity on the interface $v^d$ induced by a moving dipole has the power series expansion

$$v^d(\eta) = t v_1^d + t^3 v_3^d + \cdots \tag{4.18}$$



https://doi.org/10.1017/jfm.2026.11884 Published online by Cambridge University Press

with coefficients

$$v_1^d(x) = 4r^2(q'(x)\sin\theta - p'(x)\cos\theta), \tag{4.19}$$

$$v_3^d(x) = 4r^2(p''(x)\cos 2\theta - q''(x)\sin 2\theta) + 4r^2\big[\eta_2(x)(p'(x)\sin\theta + q'(x)\cos\theta)\big]'. \tag{4.20}$$

Replacing the unknown functions with their time expansions in the integral equations (3.5) and (3.12) for the case of a cylinder moving in the lower layer leads to the following system of recursive equations:

$$\left[I + r^2 A_0^r\right] v_n(x) - \left[H + r^2 B_0^r\right] u_n(x) = \varphi_n(x), \tag{4.21}$$

$$v_n(x) + H w_n(x) = \psi_n(x), \tag{4.22}$$

where $I$ is the identity operator, and the non-homogeneous terms $\varphi_n$ and $\psi_n$ can be evaluated explicitly via the coefficients up to the $(n-1)$th order by

$$\varphi_n(x) = v_n^d(x) + \sum_{j=1}^{n}\Big(B_j u_{n-j}(x) - A_j v_{n-j}(x)\Big) + r^2\sum_{j=1}^{n}\Big(B_j^r u_{n-j}(x) - A_j^r v_{n-j}(x)\Big), \tag{4.23}$$

$$\psi_n(x) = \sum_{j=1}^{n}\Big(A_j v_{n-j}(x) - B_j w_{n-j}(x)\Big). \tag{4.24}$$

Equations (4.5), (4.6), (4.21) and (4.22) form the full set of recursive equations for the unknown coefficients $(\eta_n, u_n, w_n, v_n)$. Using (4.6), the pair of integral equations (4.21) and (4.22) can be rewritten in operator form for a vector-valued unknown function $\boldsymbol{v}_n = (v_n, w_n)$:

$$\Big(I + \frac{r^2}{1+\rho}\boldsymbol{A}_0^r\Big)\boldsymbol{v}_n(x) = \boldsymbol{f}_n(x), \tag{4.25}$$

where

$$\boldsymbol{A}_0^r = \begin{pmatrix} A_0^r & -\rho B_0^r \\ HA_0^r & -\rho H B_0^r \end{pmatrix}, \quad \boldsymbol{f}_n(x) = \frac{1}{1+\rho}\begin{pmatrix} H\phi_n + \varphi_n + \rho\psi_n + r^2 B_0^r\phi_n \\ -\phi_n + H\varphi_n - H\psi_n + r^2 H B_0^r\phi_n \end{pmatrix}. \tag{4.26}$$

Equation (4.25) is the Fredholm integral equation of the second kind, and is uniquely solvable for small values of the parameter $r$ and a given density parameter $0 \leqslant \rho < 1$ (Trikomi 1957), that is, in the case of a sufficiently large submergence depth of the cylinder. The solution is found iteratively using the convergent Neumann series

$$\boldsymbol{v}_n(x) = \sum_{k=0}^{\infty}\frac{(-1)^k r^{2k}}{(1+\rho)^k}\Big\{\boldsymbol{A}_0^r\Big\}^k \boldsymbol{f}_n(x). \tag{4.27}$$

We now have a recursive procedure to construct the small-time asymptotic solution. By solving the system of equations (4.5), (4.6), (4.21) and (4.22) sequentially for different orders $n$, we find the first four coefficients for the interface displacement:

$$\eta_1(x) = 0, \tag{4.28}$$

$$\eta_2(x) = (1+a)\left(r^2 - \frac{ar^4}{4}\right)(q'(x)\sin\theta - p'(x)\cos\theta) + O(r^6), \tag{4.29}$$



https://doi.org/10.1017/jfm.2026.11884 Published online by Cambridge University Press

$$\eta_3(x) = 0, \tag{4.30}$$

$$\begin{aligned}\eta_4(x) = {} & \frac{1+a}{2}\left(r^2 - \frac{ar^4}{4}\right)\left[\left(\frac{\lambda a}{6}\cos\theta - \sin 2\theta\right)q''(x) + \left(\cos 2\theta + \frac{\lambda a}{6}\sin\theta\right)p''(x)\right] \\ & + \frac{a(1+a)}{8}r^4\left[\left(\cos 2\theta + \frac{\lambda(1+a)}{6}\sin\theta\right)q'(x)\right. \\ & \left. + \left(\sin 2\theta - \frac{\lambda(1+a)}{6}\cos\theta\right)p'(x)\right] \\ & + \frac{1+a}{8}r^4\left[\left(\frac{1}{3} + \frac{1}{3}a - \frac{2}{9}a^2\right)\left(p^{(4)}(x)\cos 2\theta - q^{(4)}(x)\sin 2\theta\right)\right. \\ & \left. + a\left(a + \frac{1}{3}\right)p''(x) - a\left(a + \frac{4}{3}\right)q'(x)\right] + O(r^6).\end{aligned} \tag{4.31}$$

Detailed calculation for the above-mentioned solution can be found in Appendices A and B. It is worth noting that for $a = 1$, (4.28)–(4.31) describe the shape of the free surface, as predicted by Kostikov & Makarenko (2018) for a cylinder moving in a one-layer fluid. In the limit of a weakly stratified fluid, when the densities of the two fluids are almost equal ($a \to 0$), the contribution of the nonlinear terms of order $r^4$ is reduced to zero, while the leading linear terms of order $r^2$ are reduced by half compared with the limiting case of free surface flow ($a = 1$).

In the case of a cylinder moving in the upper layer of a two-layer fluid, the coefficients can be derived following the same principle:

$$\eta_1(x) = 0, \tag{4.32}$$

$$\eta_2(x) = (1-a)\left(r^2 + \frac{ar^4}{4}\right)(q'(x)\sin\theta + p'(x)\cos\theta), \tag{4.33}$$

$$\eta_3(x) = 0, \tag{4.34}$$

$$\begin{aligned}\eta_4(x) = {} & -\frac{1-a}{2}\left(r^2 + \frac{ar^4}{4}\right)\left[\left(\sin 2\theta + \frac{\lambda a}{6}\cos\theta\right)q''(x) + \left(\cos 2\theta - \frac{\lambda a}{6}\sin\theta\right)p''(x)\right] \\ & + \frac{a(1-a)}{8}r^4\left[\left(\cos 2\theta + \frac{\lambda(1-a)}{6}\sin\theta\right)q'(x)\right. \\ & \left. - \left(\sin 2\theta - \frac{\lambda(1-a)}{6}\cos\theta\right)p'(x)\right] \\ & + \frac{1-a}{8}r^4\left[\left(-\frac{1}{3} + \frac{1}{3}a + \frac{2}{9}a^2\right)\left(p^{(4)}(x)\cos 2\theta + q^{(4)}(x)\sin 2\theta\right)\right. \\ & \left. - a\left(a - \frac{1}{3}\right)p''(x) + a\left(a - \frac{4}{3}\right)q'(x)\right].\end{aligned} \tag{4.35}$$

It is evident that in the case of a one-layer fluid with a free surface ($a = 1$), the coefficients (4.33) and (4.35) turn to zero and the interface disappears. In a weakly stratified fluid ($a \to 0$), contribution of nonlinear terms with $r^4$ is reduced to zero, and the leading linear terms with $r^2$ start to dominate the flow with increasing magnitude.

Ideally, the equivalence of solutions (4.28)–(4.31) and (4.32)–(4.35) must obey a certain conversion rule, in accordance with the inversion of the direction of the gravity force relative to the interface. Comparing the above-mentioned coefficients, we can conclude that to the first order of accuracy, the solution for the cylinder in the upper layer (4.33) can be obtained from the solution for the cylinder in the lower layer (4.29) by inverting



https://doi.org/10.1017/jfm.2026.11884 Published online by Cambridge University Press

the signs of parameter $a$ and the differentiated kernel function $p'(x)$. A different principle applies to the next order of accuracy. Similarly, coefficient (4.35) differs from coefficient (4.31) in the signs of parameter $a$, and the differentiated kernel functions $p'(x)$ and $q''(x)$, but not in a general way. This is due to a cancellation effect occurring as a result of multiple conversions at this order.

Equations (4.28)–(4.35) provide explicit analytical representations of the instantaneous shape of the interface of a two-layer fluid, when a circular cylinder starts to move with constant acceleration from rest in one of the layers. The flow regimes are determined by four parameters: the radius of the cylinder ($r$), the direction of motion ($\theta$), the rate of acceleration ($\lambda$) and the relative density ratio (the Atwood number $a$). Certain limitations on the range of values for parameter $\lambda$ should be imposed to avoid a growing cavity behind the body. A situation when the fluid detaches from the body surface, forming the cavity, can occur when a cylinder is abruptly displaced from its initial position. The safe range for the Froude number, for which the fluid pressure does not decrease below a certain level around a circular cylinder in a one-layer fluid, was established by Norkin (2012). In our notation, this bound corresponds to the condition $\lambda > 0.78$. To the best of our knowledge, there is no known study of this kind of cavitation phenomenon for a two-layer fluid. In the subsequent analysis, we assume that the bound $\lambda > 0.78$ holds for flow without cavity formation.

The asymptotic solution (4.28)–(4.35) has been obtained under the assumption of small time and small radius, using infinite series with respect to the corresponding parameters. Hence, the validity of the results is limited to the analysis of small obstacles within a short time interval. Earlier, Pardo & Nedic (2021) extended our asymptotic solution for a one-layer fluid (Kostikov & Makarenko 2018) to study cylinders of arbitrary radius. They used an iterative numerical algorithm to solve the boundary integral equation on the free surface to calculate coefficients up to the eighth order, valid without any assumptions on the size of the cylinder. By comparing with their numerical calculations, they established that the fourth-order analytical solution (4.28)–(4.31) with $a = 1$ works well for cylinders of radius $r \leqslant 0.5$ and for the time interval $t < 0.8$. They investigated the temporal validity of the time expansions depending on the number of calculated terms and concluded that the the fourth-order solution deviates from the eighth-order solution by less than 5 % for $t < 0.6$ when $\lambda = 5$ and for $t < 0.85$ when $\lambda = 0.1$. Later, Pardo *et al.* (2022) validated the analytical model of Kostikov & Makarenko (2018) and semi-analytical model of Pardo & Nedic (2021) experimentally. Solution (4.28)–(4.35) generalises the results of Kostikov & Makarenko (2018) to a two-layer fluid. Based on analogy with the one-layer free surface problem, a similar range of applicability with respect to the radius $r$ and time $t$ may be anticipated. However, this validity range remains an inferred estimate, since it has not yet been independently demonstrated or validated for the present two-layer problem.

## 5. Hydrodynamic forces

The vector of hydrodynamic forces $(X, Y)$ acting on the cylinder, accelerating in the lower layer of a two-layer fluid, can be found from Sedov's formula (Sedov 1965):

$$X(t) + iY(t) = \pi r^2 \ddot{z}_c(t) + i\frac{\mathrm{d}}{\mathrm{d}t}\int_S z F_+(z,t)\,\mathrm{d}z + \overline{\frac{i}{2}\int_S (F_+(z,t))^2\,\mathrm{d}z}, \tag{5.1}$$

where $S$ is the contour of the cylinder and $F(z,t) = U_+ - iV_+$ is the complex velocity of the fluid in the lower layer $\Omega_+$. Since Sedov's formula (5.1) and its subsequent evaluation



https://doi.org/10.1017/jfm.2026.11884 Published online by Cambridge University Press

are invariant with respect to the location of the cylinder relative to the interface, the function $F(z,t)$ will herafter be written without a subscript.

To calculate the contour integrals in (5.1), we use representation (3.4) for function $F(z,t)$, introduced in § 3. For clarity of the subsequent discussion, we reproduce this formula here:

$$2\pi i F(z,t) = \int\limits_{\Gamma(t)} \frac{F(\zeta,t)\,\mathrm{d}\zeta}{\zeta - z} + \frac{r^2}{(z-z_c(t))^2}\overline{\int\limits_{\Gamma(t)} \frac{F(\zeta,t)\,\mathrm{d}\zeta}{\zeta - z_*(t)}} + \frac{\gamma}{z-z_c(t)} + \frac{2\pi i r^2 \dot{z}_c(t)}{(z-z_c(t))^2}. \tag{5.2}$$

By expanding the complex quantity $z_*(t) = z_c(t) + r^2/\overline{z - z_c(t)}$ in powers of $r$ in the last integral term of formula (5.2), it can be rewritten as a multipole expansion:

$$F(z,t) = F^{(0)}(z,t) + \frac{1}{2\pi i}\frac{\gamma}{z-z_c(t)} + \frac{r^2\dot{z}_c(t)}{(z-z_c(t))^2} - \frac{r^2}{(z-z_c(t))^2}\sum_{n=0}^{\infty}\frac{r^{2n}\overline{F^{(n)}(z_c,t)}}{(z-z_c(t))^n}, \tag{5.3}$$

where

$$F^{(n)}(z,t) = \frac{1}{2\pi i}\int\limits_{\Gamma(t)}\frac{F(\zeta,t)\,\mathrm{d}\zeta}{(\zeta-z)^{n+1}} = \frac{1}{n!}\frac{\mathrm{d}^n}{\mathrm{d}z^n}F^{(0)}(z,t), \quad n = 0,\,1,\,\ldots \tag{5.4}$$

For each $n = 0,\,1,\,\ldots$, the function $F^{(n)}(z,t)$ is analytic in the fluid layer, occupied by the cylinder, that is, for $z \in \{z \mid \mathrm{Im} z < \eta(x,t)\}$. From definition (5.4), it follows by the residue theorem:

$$\frac{1}{2\pi i}\int\limits_{S}\frac{F^{(0)}(\zeta,t)\,\mathrm{d}\zeta}{(z-z_c(t))^{n+1}} = \mathrm{Res}_{z=z_c(t)}\left(\frac{F^{(0)}(z,t)}{(z-z_c(t))^{n+1}}\right) = F^{(n)}(z_c,t). \tag{5.5}$$

Substituting the multipole expansion (5.3) into Sedov's formula (5.1) and using the residue theorem, we obtain the following formula for zero circulation ($\gamma = 0$):

$$\frac{X(t)+iY(t)}{2\pi r^2} = -\frac{\ddot{z}_c(t)}{2} + \frac{\mathrm{d}\overline{F^{(0)}(z_c(t),t)}}{\mathrm{d}t} - \overline{\dot{z}_c(t)F^{(1)}(z_c(t),t)} + \sum_{n=0}^{\infty} r^{2n} F^{(n)}(z_c(t),t),\,\overline{F^{(n+1)}(z_c(t),t)}. \tag{5.6}$$

Golikov & Makarenko (2022, 2024) introduced the representation (5.6) for the unsteady forces in powers of $r$ for both forced and free motions of the cylinder in a one-layer fluid. They observed that the first term in the total force in formula (5.6) is responsible for the added mass of the cylinder during its unsteady motion in an unbounded fluid. The second term corresponds to the integral of $zF(z,t)$ in (5.1) and reflects the unsteady nature of the process. The last term, which depends bilinearly on the coefficients $F^{(n)}$, represents the integral of $(F(z,t))^2$ in (5.1) and is also present in the Blasius–Chaplygin formula for nonlinear loads in the case of stationary motion. A key property of the representation (5.6) is that it depends only on the instantaneous shape of the interface $\eta(x,t)$, the velocity components $u(x,t)$, $w(x,t)$, $v(x,t)$ on it, and the trajectory of the cylinder $z_c(t)$.

The function $F^{(n)}(z,t)$, defined by the boundary integral (5.4), can be expanded in powers of $t$, using the series for the velocity componenets $u_n(x)$ and $v_n(x)$ and the



https://doi.org/10.1017/jfm.2026.11884 Published online by Cambridge University Press

interface displacement $\eta_n(x)$:

$$2\pi i F^{(n)}(z,t) = t\int_{-\infty}^{+\infty}\frac{(iv_1(x)-u_1(x))\,\mathrm{d}x}{(x-z)^{n+1}} + t^3\int_{-\infty}^{+\infty}\frac{(iv_3(x)-u_3(x))\,\mathrm{d}x}{(x-z)^{n+1}} + (n+1)t^3\int_{-\infty}^{+\infty}\frac{(v_1(x)+iu_1(x))\eta_2(x)\,\mathrm{d}x}{(x-z)^{n+2}} + O\big(t^5\big). \tag{5.7}$$

By calculating the integrals in (5.7) up to third order in time $t$ and fourth order in radius $r$, and substituting the result into (5.6), we obtain the following asymptotic formula for the hydrodynamic force on a cylinder moving in the lower layer of a two-layer fluid at an arbitrary angle to the interface:

$$\frac{X(t)+iY(t)}{2\pi r^2} = -e^{i\theta} - 2r^2 a\left(1-\frac{ar^2}{4}\right)\left[\frac{e^{i\theta}}{(t^2e^{-i\theta}+2i)^2} + t^2\frac{6e^{2i\theta}-i\lambda(1+a)e^{i\theta}}{(t^2e^{-i\theta}+2i)^3}\right] - \frac{ar^4}{2}\left[\frac{6iae^{2i\theta}+\lambda a(1+a)e^{i\theta}-2i(3a^2+7a+1)}{2(t^2e^{-i\theta}+2i)^2} + \frac{2(3a^2+4a+1)}{(t^2e^{-i\theta}+2i)^3} + \frac{16a}{(t^2e^{-i\theta}+2i)^3(t^2e^{i\theta}-2i)^2} + \frac{16(-a^2+2a+3)e^{2i\theta}}{(t^2e^{-i\theta}+2i)^5}\right]t^2 + O\big(t^4+r^6\big). \tag{5.8}$$

The detailed calculation of the integrals in (5.7) can be found in Appendices A and B.

Using the same methodology, the asymptotic formula for the hydrodynamic forces on a cylinder in the upper layer can be derived as

$$\frac{X(t)+iY(t)}{2\pi r^2} = -e^{i\theta} + 2ar^2\left(1+\frac{ar^2}{4}\right)\left[\frac{e^{i\theta}}{(t^2e^{-i\theta}-2i)^2} + t^2\frac{6e^{2i\theta}-i\lambda(1-a)e^{i\theta}}{(t^2e^{-i\theta}-2i)^3}\right] + \frac{ar^4}{2}\left[\frac{6iae^{2i\theta}+\lambda a(1-a)e^{i\theta}+2i(3a^2-7a+1)}{2(t^2e^{-i\theta}-2i)^2} + \frac{2(3a^2-4a+1)}{(t^2e^{-i\theta}-2i)^3} - \frac{16a}{(t^2e^{-i\theta}-2i)^3(t^2e^{i\theta}+2i)^2} + \frac{16(a^2-2a+3)e^{-2i\theta}}{(t^2e^{-i\theta}-2i)^5}\right]t^2 + O\big(t^4+r^6\big). \tag{5.9}$$

Comparing the asymptotics (5.8) and (5.9) for the hydrodynamic forces, we conclude that (5.8) can be transformed into (5.9) almost completely by changing the sign of the parameter $a$. The transformation of the higher-order terms in the expansion formulae is difficult to trace because of the multiple overlaps of various effects, such as gravity, the position of the cylinder relative to the interface and the direction of motion.

Neglecting the terms of the order $r^4$ in (5.8) and expanding the remaining terms in powers of $t$, we obtain the leading-order asymptotic representation for the hydrodynamic force:

$$\frac{X(t)+iY(t)}{2\pi r^2} = -e^{i\theta} + \frac{ar^2}{2}e^{i\theta} - \frac{3ar^2}{2}\left(ie^{2i\theta} + \frac{(1+a)\lambda}{6}e^{i\theta}\right)t^2 + O(t^4+r^4). \tag{5.10}$$

It is interesting to observe that the structure of the asymptotics (5.10) inherits the structure of the coefficients (4.29) and (4.31) in the time expansion of the interface deformations. The second and third terms in (5.10) represent the wave-induced forces on the cylinder and, in the limit of a homogeneous fluid ($a \to 0$), vanish, making the force almost uniform.



https://doi.org/10.1017/jfm.2026.11884 Published online by Cambridge University Press

Analysis of (5.10) shows that the hydrodynamic force acting on the accelerated cylinder is generally reduced in a two-layer fluid ($0 < a < 1$) compared with a homogeneous one-layer fluid ($a = 1$). The specific influence of the density parameter $a$ on the forces for various directions of cylinder motion will be examined in detail in § 7.

## 6. Comparisons with alternative theories

The amount of research on unsteady interface flow in a two-layered fluid in the presence of an obstacle is limited and, to the best of our knowledge, there is no rigorous experimental or numerical validation of the asymptotic solution obtained here. Theoretical models for a one-layered fluid, which are more extensively represented in the literature, are mostly concerned with steady-state solutions to diffraction and radiation problems. Most existing models for the initial stage of wave motion investigate free surface deformations that occur when a cylinder starts to move impulsively with constant velocity (Haussling & Coleman 1979) or are produced by constant body motion after an initial acceleration period (Telste 1987; Gorlov 2000). Laboratory experiments focus mainly on water-entry and water-exit problems (Greenhow 1988; Moyo & Greenhow 2000; Vincent *et al.* 2026). It is therefore problematic to bring our theoretical model, specifically designed for initial perturbations of the interface, in strict correspondence with the limited available data, even for a one-layer fluid. Only recently, Pardo *et al.* (2022) conducted the first experiments to estimate the prediction time of their small-time asymptotic solution obtained by a recursive semi-analytical method (Pardo & Nedic 2021). Their method extended the asymptotic solution of Kostikov & Makarenko (2018) to cylinders of arbitrary radius under general submersion motions and thus provided solid experimental validation of the theoretical approach used in this paper. In this section, we provide the primary consistency check of our results for a two-layer fluid by comparing them with the exact solution of linear wave theory.

### 6.1. *Linear water wave theory*

In the theoretical solution of the linear problem of internal waves generated by a moving circular cylinder, the body can be modelled as a point dipole with a time-dependent moment, turning on at time $t = 0$. The position of the dipole is determined by the trajectory of the cylinder $(x_c(t),\ y_c(t))$ and its intensity is given by $\mu(t) = -2\pi r^2 U_c(t)$, where $U_c(t)$ is the speed of the cylinder. Following the approach proposed by Bukreev *et al.* (1983, 1986), the equations of motion for a cylinder below the interface in a two-layer fluid can be formulated in terms of the vertical fluid velocities in two layers:

$$\Delta V_- = 0, \quad y > 0, \tag{6.1}$$

$$\Delta V_+ = \mu(t)\delta(x - x_c(t))\frac{\partial}{\partial y}\delta(y - y_c(t)), \quad y < 0 \tag{6.2}$$

$$V_- = V_+, \quad y = 0, \tag{6.3}$$

$$\frac{\partial^3 V_-}{\partial t^2 \partial y} - \lambda\frac{\partial^2 V_-}{\partial x^2} = \frac{1}{\rho}\left(\frac{\partial^3 V_+}{\partial t^2 \partial y} - \lambda\frac{\partial^2 V_+}{\partial x^2}\right), \quad y = 0, \tag{6.4}$$

$$V_\pm \to 0. \quad y \to \pm\infty. \tag{6.5}$$

Here, $\delta$ is the Dirac delta function and the parameter $\lambda$ appears as a non-dimensional replacement for the gravitational acceleration $g$. Once the system of equations (6.1)–(6.5) has been solved, the interface deformation can be found from the formula:

$$\frac{\partial \eta}{\partial t} = V_-, \quad y = 0. \tag{6.6}$$



https://doi.org/10.1017/jfm.2026.11884 Published online by Cambridge University Press

To solve the initial-boundary value problem (6.1)–(6.5), we apply the Fourier transform with respect to the spatial variable $x$ and the Laplace transform with respect to the time variable $t$:

$$\hat{V}(k, y, s) = \int_0^\infty e^{-st}\,\mathrm{d}t \int_{-\infty}^{\infty} V(x, y, t)e^{-ikx}\,\mathrm{d}x, \tag{6.7}$$

where the variable $k$ is real and the real part of the complex variable $s$ is positive. The transformed problem takes the form of a second-order boundary value problem for $\hat{V}(k, y, s)$:

$$\hat{V}_-'' - k^2\hat{V}_- = 0, \quad y > 0 \tag{6.8}$$

$$\hat{V}_+'' - k^2\hat{V}_+ = \int_0^\infty \mu(t)\exp(-st - ikx_c(t))\frac{\partial}{\partial y}\delta(y - y_c(t))\,\mathrm{d}t, \quad y < 0 \tag{6.9}$$

$$\hat{V}_- = \hat{V}_+, \quad y = 0 \tag{6.10}$$

$$s^2\hat{V}_-' + \lambda k^2\hat{V}_- = \frac{1}{\rho}\left(s^2\hat{V}_+' + \lambda k^2\hat{V}_+\right), \quad y = 0 \tag{6.11}$$

$$\hat{V}_\pm \to 0, \quad y \to \pm\infty. \tag{6.12}$$

Here, the prime denotes differentiation with respect to $y$. Once the problem (6.8)–(6.12) is solved, the transformed displacement of the interface from the unperturbed flat position can be found from the formula

$$\hat{\eta}(k, s) = \frac{\hat{V}_-(k, 0, s)}{s} = \frac{(1 + a)s}{s^2 + a\lambda k}\int_0^\infty \mu(t)\exp\left(-st - ikx_c(t) + ky_c(t)\right)\mathrm{d}t. \tag{6.13}$$

The solution of the original problem is found by taking the inverse Fourier and Laplace transforms of (6.13)

$$\eta(x, t) = \frac{1}{2\pi}\int_{-\infty}^{\infty}\mathrm{d}k\int_0^\infty \mu(\tau)\exp(ik(x - x_c(\tau)) - ky_c(\tau))H(k, t, \tau)\,\mathrm{d}\tau, \tag{6.14}$$

where

$$H(k, t, \tau) = \frac{1}{2\pi i}\int_{c-i\infty}^{c+i\infty}\frac{(1 + a)se^{s(t-\tau)}}{s^2 + a\lambda k}\,\mathrm{d}s = a\cos\left(\sqrt{a\lambda k}(t - \tau)\right). \tag{6.15}$$

The integral in (6.15) converges if the real part of $s$ exceeds some minimum value, set as $c_0$, such that all singularities of the integrand $s = \pm ia\lambda k$ lie to the left of the line $\mathrm{Re}(s) = c_0$. The inverse Laplace transform given in (6.15) then exists for all $c > c_0$ (see Andrews & Shivamoggi 1998). Substituting the expression (6.15) into the integral formula (6.14) and taking into account that function $H(k, t, \tau)$ is non-zero only for $\tau < t$, we obtain the final expression for the interface displacement of the linear theory:

$$\eta(x, t) = 2r^2(1 + a)\int_0^\infty k\,\mathrm{d}k \cdot \int_0^t e^{-ky_c(\tau)} \times \left[\dot{x}_c(\tau)\sin k(x - x_c(\tau)) - \dot{y}_c(\tau)\cos k(x - x_c(\tau))\right]\cos\sqrt{a\lambda k}(t - \tau)\,\mathrm{d}\tau. \tag{6.16}$$



https://doi.org/10.1017/jfm.2026.11884 Published online by Cambridge University Press

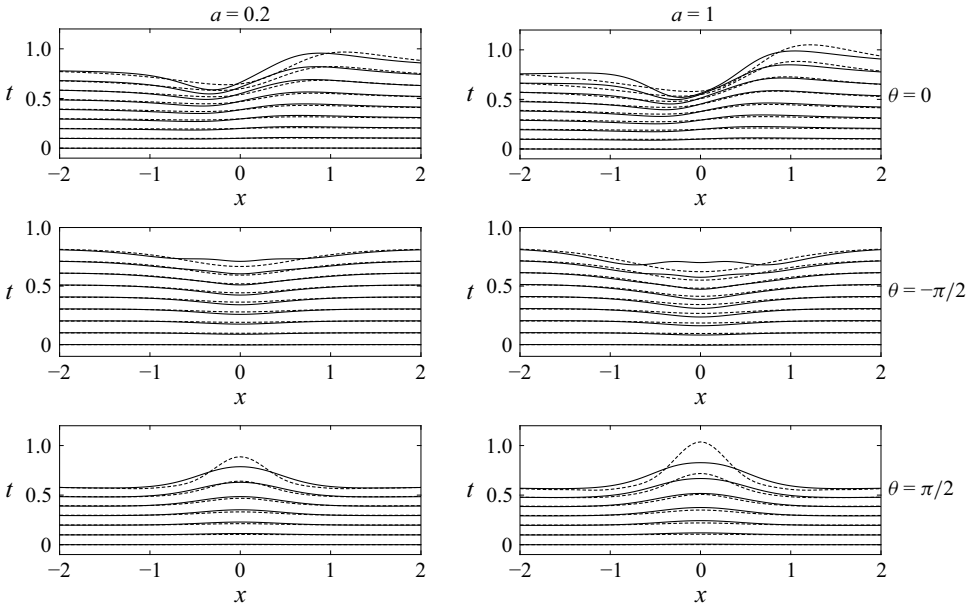



Figure 2. Snapshots of the interface for a cylinder of radius $r = 0.5$, moving in different directions in the lower layer of a two-layered fluid with $\lambda = 3.5$, predicted by higher-order asymptotic solution (4.29)–(4.31) (solid line) and by solution of the linear theory (6.16) (dashed line).

Following the same principle, we can derive the interface displacement for a cylinder moving in the upper layer, see Bukreev *et al.* (1983). In this case, the resulting interface displacement differs from (6.16) only by the multiplication constant $1 - a$.

Stepanyants & Sturova (2021) used the same principle of replacing a submerged body with a dipole to describe the elastic waves on the floating elastic ice sheet caused by the motion of a circular cylinder. They showed that small-amplitude waves in the linear approximation are not too sensitive to the shape of a moving body, and the correction to the circular shape of the cylinder by an ice sheet is negligible provided that the cylinder moves relatively slow or sufficiently far from the interface. Similarly, the dipole approximation can be justified for the motion of a cylinder below the free surface or in a two-layered fluid. In fact, this approach has been used extensively (Bukreev *et al.* 1983, 1986) to describe wave generation by the unsteady motion of a circular cylinder in a two-layer fluid. Earlier, Havelock (1927) and Sretensky (1937) applied the method of images in the linear problem of water waves to describe the free surface flow caused by the horizontal motion of a cylindrical body, and arrived at the same integral formula (6.16) for the case $a = 1$.

A comparison of the derived asymptotic formula for the interface displacement (4.28)–(4.31) with its analogue from the linear wave theory (6.16) reveals that, in both cases, the parameter $(1 + a)$ appears as a multiplication factor for the entire solution. Furthermore, the parameter $a$ specifically affects the term with $\lambda$, which is related to the Froude number.

Figure 2 compares the higher-order asymptotic solution given by (4.28)–(4.31) with the solution from linear wave theory (6.16) for a cylinder moving in the lower layer of a two-layer fluid. The figure shows the interface displacement at regular time intervals for three directions of cylinder motion: horizontal ($\theta = 0$), vertical submersion ($\theta = -\pi/2$), vertical emersion ($\theta = \pi/2$). Two distinct cases are displayed: a small density difference ($a = 0.21$) and free surface flow ($a = 1$), to highlight features specific to a two-layered fluid. Figure 2 demonstrates that at early times ($t < 0.5$), the agreement between the two solutions is



https://doi.org/10.1017/jfm.2026.11884 Published online by Cambridge University Press

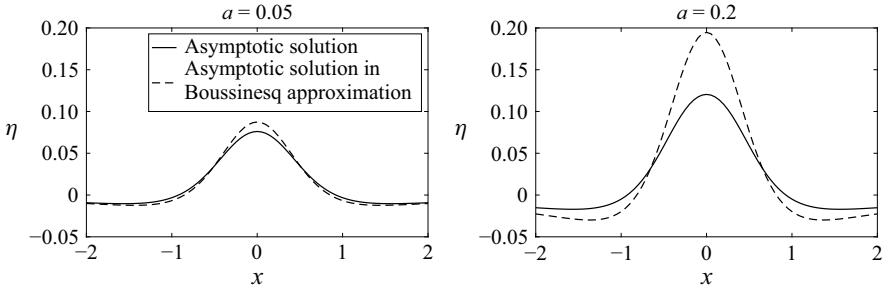



Figure 3. Interface $y = \eta(x, t)$ of a two-layer fluid with different density difference for a circular cylinder of radius $r = 0.4$ and parameter $\lambda = 10$, moving vertically upwards in the lower layer ($x_c = 0$, $y_c = -1 + t^2$).

reasonably good. A further increase in time leads to growing discrepancies, which may be attributed to the increasing influence of nonlinear effects or the limited validity range of the asymptotic solution. As noted previously, agreement persists for a longer duration in a two-layered fluid with a small density difference, which is consistent with the structure of the asymptotic solution. It is also noteworthy that good agreement is maintained until later times for the case of horizontal motion near the wave crest pushed ahead by the cylinder.

### 6.2. *The Boussinesq approximation*

In the Boussinesq approximation, commonly used to describe the internal waves in a weakly stratified fluid, the densimetric parameter $\lambda^* = (1 - \rho)\lambda$ is introduced, where the non-dimensional parameter $\rho = \rho_-/\rho_+$ is the density ratio. Taking the limit $\rho \to 1$, we can reproduce the boundary differential equations (3.2) and (3.3) for a weakly stratified two-layer fluid in the form:

$$\eta_t = v, \quad u_t - w_t + \frac{1}{2}\frac{\partial}{\partial x}\left(\frac{u^2 - 2\eta_x v(u - w) - w^2}{1 + \eta_x^2}\right) + \lambda^* \eta_x = 0. \tag{6.17}$$

The integral equations (3.5) and (3.12), which complement the system (6.17), remain unchanged, as they contain no information about the density difference. Following the theoretical approach, discussed earlier, we obtain the small-time asymptotic solution for the interface displacement in the Bouassinesq approximation. The coefficients in the time expansion of this solution are given by

$$\eta_1(x) = 0, \quad \eta_2(x) = r^2(q'(x)\sin\theta - p'(x)\cos\theta), \quad \eta_3(x) = 0,$$
$$\eta_4(x) = \frac{r^2}{2}\left[\left(\frac{\lambda^*}{12}\cos\theta - \sin 2\theta\right)q''(x) + \left(\cos 2\theta + \frac{\lambda^*}{12}\sin\theta\right)p''(x)\right]$$
$$+ \frac{r^4}{24}\left[\frac{\lambda^*}{4}\left(q'(x)\sin\theta - p'(x)\cos\theta\right) + \left(p^{(4)}(x)\cos 2\theta - q^{(4)}(x)\sin 2\theta\right)\right]. \tag{6.18}$$

The vector of hydrodynamic forces (5.8) in the Boussinesq approximation reduces to

$$\frac{X + iY}{2\pi r^2} = -e^{i\theta} + it^2 r^2 \frac{\lambda_* e^{i\theta}}{(t^2 e^{-i\theta} + 2i)^3}. \tag{6.19}$$

Figure 3 illustrates the good agreement between the two high-order asymptotic solutions, obtained with and without Boussinesq approximation, when the density difference is sufficiently small. As the density stratification intensifies, as shown in



https://doi.org/10.1017/jfm.2026.11884 Published online by Cambridge University Press

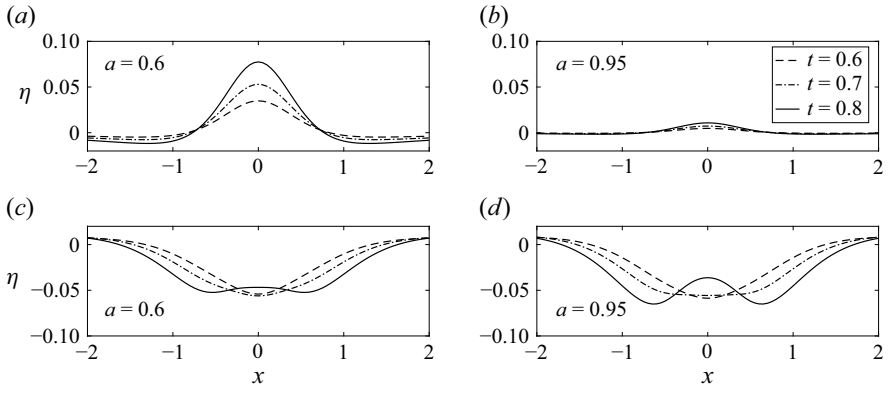



Figure 4. Snapshots of the interface $y = \eta(x, t)$ of a two-layer fluid at three successive moments of time for the cylinder of radius $r = 0.4$ and parameter $\lambda = 4$, moving ($a$, $b$) vertically upwards in the upper layer ($x_c = 0$, $y_c = 1 + t^2$) and ($c$, $d$) vertically downwards in the lower layer ($x_c = 0$, $y_c = -1 - t^2$).

figure 3($b$), the asymptotic solution based on the Boussinesq approximation becomes ineffective, as it substantially overestimates the amplitude of the interface flow.

## 7. Analysis of the asymptotic solution

In this section, we study the factor of a two-layer fluid in the initial stage of the wave–structure interaction. We investigate the effect of the density stratification parameter, namely Atwood number $a$, on the dynamics of the interface flow of a two-layer fluid and the hydrodynamic forces exerted on the moving body. It is interesting to compare the initial perturbations formed on the interface of a two-layer fluid as a result of the unsteady motion of a cylinder in the lower and upper layers.

### 7.1. *Motion away from the interface*

Figures 4($a$, $b$) and 4($c$, $d$) show the evolution of the interface with time when the cylinder starts to move vertically away from the interface in the upper and lower layer, respectively. Two distinct configurations of a two-layer fluid with intermediate ($a = 0.5$) and strong ($a = 0.95$) stratification are displayed. Figure 4($a$, $b$) shows that the initially planar interface is entrained by the elevating cylinder in the upper layer and forms a central elevation zone, the magnitude of which is governed by the density difference. When the density difference is large, the interface is almost insensitive to the action of a moving body in the upper layer. Similarly, a central depression zone forms above a submerging cylinder in the lower layer, but the morphology of the wave is quite different. According to figure 4($c$, $d$), at later times, the interface flattens and evolves into a vertical jet, which occurs as the result of the collision of small-scale waves propagating towards each other along the moving curvilinear interface. When the density difference is small, the jet forms at later times and cannot be fully observed within the validity period of the asymptotic solution. The variation in the wave response observed in figure 4 for the two different stratification cases is due to the fact that the interface of a two-layer fluid experiences different excessive pressures from the top layer, which alleviates the wave motion generated by a moving obstacle.

Figures 5($a$) and 5($b$) compare the hydrodynamic forces predicted by (5.8) and (5.9), respectively, acting on the cylinder in the situations depicted in figure 4. The vertical foce acting on the lower cylinder grows with time, reaching an extremum at the point where the



https://doi.org/10.1017/jfm.2026.11884 Published online by Cambridge University Press

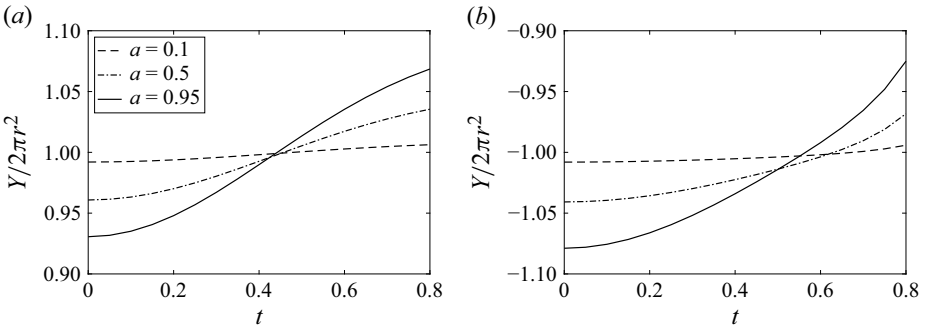



Figure 5. Vertical force on a cylinder of radius $r = 0.4$ and $\lambda = 4$, moving vertically ($a$) downwards in the lower layer ($x_c = 0$, $y_c = -1 - t^2$) and ($b$) upwards in the upper layer ($x_c = 0$, $y_c = 1 + t^2$) of a two-layered fluid with different density difference.

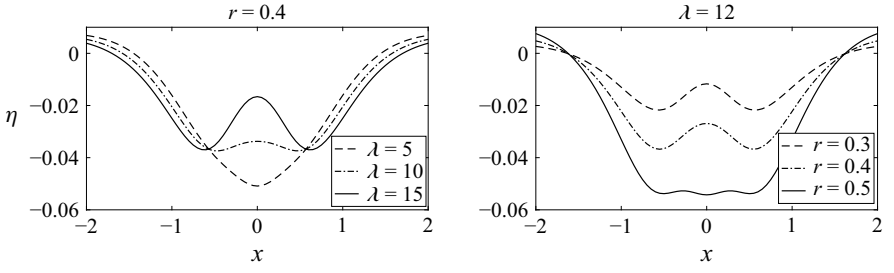



Figure 6. Snapshots of the interface $y = \eta(x, t)$ of a two-layer fluid ($a = 0.4$) generated by vertical submersion of the cylinder in the lower layer ($x_c = 0$, $y_c = -1 - t^2$) of different radii $r$ and parameter $\lambda$ at time $t = 0.7$.

second-order and fourth-order terms come into balance and the jet forms at the interface. The rate of growth is larger for stronger stratification. The force on the upper cylinder experiences a similar growing trend, but without reaching an extremum.

Figure 6 shows representative instantaneous profiles of the interface as affected by variation in input parameters, such as the square of the inverse Froude number $\lambda$ and the non-dimensional cylinder radius $r$. According to figure 6, the parameter $\lambda$, which is related to the acceleration rate of the body and its submergence depth, determines the characteristic shape of the interface. Over time, the restoring force of gravity competes with the intertia of the flow, resulting in flattening of the initial elevation of the interface. An increase in cylinder size leads to a larger affected area of the interface and to the splitting of the splash-jet.

Jetting at the interface may be considered an undesirable event, as it can lead to instability of the interface flow. For example, in applications such as magnetised target fusion technology (Pardo *et al.* 2022), the interface between the magnetised plazma and the cavity must be maintained as smooth as possible. Therefore, it is beneficial to know under which conditions the jetting regime occurs. Figure 7 shows the perturbation height $\eta_0 = \eta(0, t)$ at the point on the interface above the centre of the cylinder $x = 0$ for various values of the density difference parameter ($a$), acceleration rate ($\lambda$) and cylinder size ($r$). The plots are characterised by a smooth descent followed by a reversal, where the interface stops sinking after the submerging body and changes direction. As shown in figure 7, the presence of a second layer ($a < 1$), as well as an incresed cylinder velocity, results in a



https://doi.org/10.1017/jfm.2026.11884 Published online by Cambridge University Press

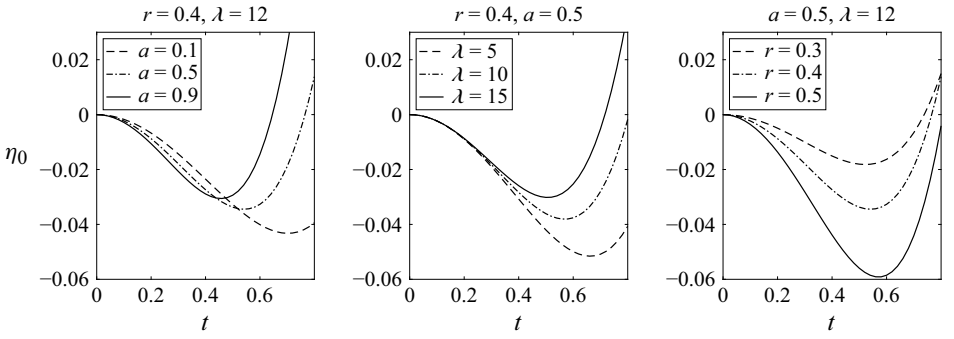



Figure 7. Vertical submersion of a circular cylinder of radius $r = 0.4$ in the lower layer of a two-layer fluid ($x_c = 0$, $y_c = -1 - t^2$): (*a*) displacement of the interface at zero point $\eta_0 = \eta(0, t)$ for $\lambda = 4$; (*b*) contour plots of critical time $t_c$ as a function of parameters $a$ and $\lambda$.

delayed and suppressed splash response of the interface. An increase in cylinder radius leads, as expected, to deeper deflection but has no effect on the turnaround point.

Investigating the extrema of the interface displacement as a function of time, $y_0 = \eta(0, t)$, yields an explicit representation for the critical time, at which the depression of the interface evolves into a reversed motion, forming a vertical jet:

$$t_c = \sqrt{\frac{1 - ar^2/4}{2 + \lambda a/3 - r^2(2 - 13a/4 + \lambda a/24 + \lambda a^2/8 - 7a^2/12)}}. \tag{7.1}$$

Neglecting terms with $r^2$ in (7.1), we obtain an approximation for the critical time valid for small-sized cylinders:

$$t_c = \sqrt{\frac{1}{2 + \lambda a/3}}. \tag{7.2}$$

Equation (7.2) demonstrates that, to leading order, the critical time is inversely proportional to the product of parameters $\lambda$ and $a$, meaning that the change of the characteristic speed of the cylinder can be compensated by proportional change in the density difference.

### 7.2. *Motion to the interface*

Figures 8(*a*, *b*) and 8(*c*, *d*) show the initial dynamics of the interface when the cylinder starts to move vertically towards the interface in the upper and lower layers, respectively. Two distinct configurations of a two-layer fluid with intermediate ($a = 0.5$) and strong ($a = 0.95$) stratification are displayed. As seen in figure 8(*a*, *b*), the downward motion of the cylinder in the upper layer induces a vertical deflection of the interface without subsequent relaxation. In figure 8(*c*, *d*), the vertical uplift of an added fluid mass by the upward motion of the cylinder in the lower layer can be observed. The disturbances induced on the interface by the upper and lower cylinders are not vertical reflections of each other. The inertial fluid layer formed on top of the cylinder can split into small-scale waves flowing around the sides of the lifting body, which does not occur when the cylinder approaches the interface from above. The overall magnitude of the disturbances produced on the interface is larger for a smaller density difference.

Figures 9(*a*) and 9(*b*) show the hydrodynamic forces predicted by (5.8) and (5.9), respectively, on the cylinder moving in the upper and lower layer of a two-layer fluid.



https://doi.org/10.1017/jfm.2026.11884 Published online by Cambridge University Press

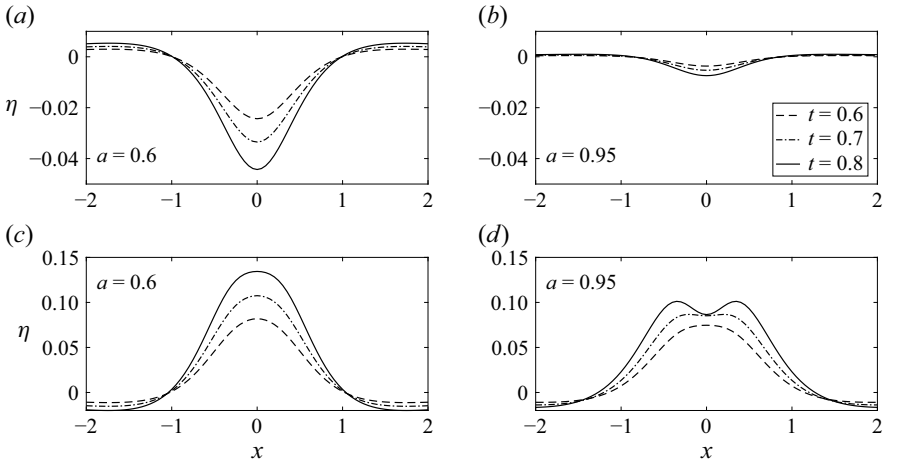



Figure 8. Snapshots of the interface $y = \eta(x, t)$ of a two-layer fluid at three successive moments of time for the cylinder of radius $r = 0.4$ and parameter $\lambda = 10$, moving $(a, b)$ vertically downwards in the upper layer ($x_c = 0$, $y_c = 1 - t^2$); $(c, d)$ vertically upwards in the lower layer ($x_c = 0$, $y_c = -1 + t^2$).

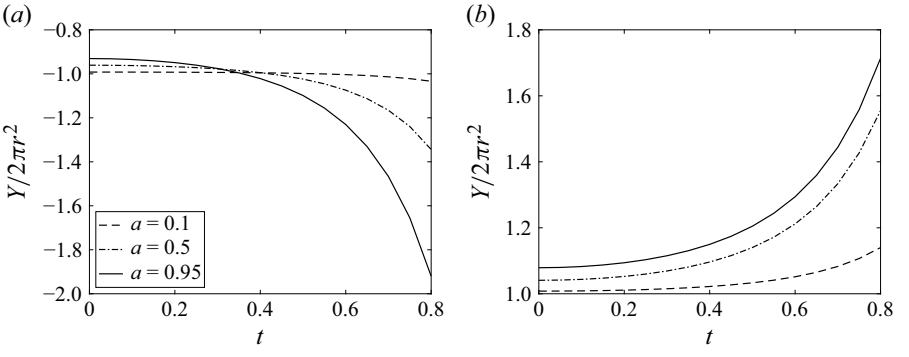



Figure 9. Vertical force on a cylinder of radius $r = 0.4$ and $\lambda = 10$, moving vertically $(a)$ upwards in the lower layer ($x_c = 0$, $y_c = -1 + t^2$) and $(b)$ downwards in the upper layer ($x_c = 0$, $y_c = -1 - t^2$) of a two-layered fluid with different density difference.

According to figure 9, the force acting on the cylinder approaching the interface from both the upper and lower layers exhibits a similar growing trend, the rate of which is highly dependent on the density stratification. When the density difference is sufficiently small, the hydrodynamic force on the cylinder moving in the lower fluid remains almost constant during the initial phase of the wave flow.

Figure 10 shows instantaneous profiles of the interface for variable input parameters $\lambda$ and $r$ when the cylinder is lifted up towards the interface in the lower layer. The general form for all conditions is a swelling of the interface as the cylinder approaches it. The volume of the swell and its surge speed depend on the radius of the cylinder $r$. According to figure 10, for a comparatively fast motion of the cylinder ($\lambda < \lambda_c$), inertial forces dominate and the interface always rises. For slow motion of the cylinder ($\lambda > \lambda_c$), the contribution of the gravity-induced outflow becomes critical and the elevation reaches a local maximum. The critical value of $\lambda_c$ is determined by the density stratification through the parameter $a$.



https://doi.org/10.1017/jfm.2026.11884 Published online by Cambridge University Press

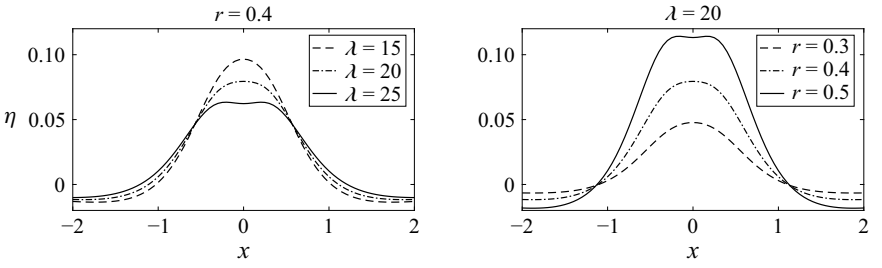



Figure 10. Snapshots of the interface $y = \eta(x, t)$ of a two-layer fluid ($a = 0.4$) generated by vertical elevation of the cylinder in the lower layer ($x_c = 0$, $y_c = -1 + t^2$) of different radius $r$ and parameter $\lambda$ at time $t = 0.7$.

## 8. Conclusion

This paper presents a closed system of integro-differential equations describing the interface flow in a two-layered fluid generated by a moving circular cylinder in either the lower or upper layer without intersecting the interface. We developed a small-time asymptotic solution for a cylinder set into motion from rest with constant acceleration in an arbitrary direction. The solution is constructed as a series expansion in powers of time and a small parameter representing the non-dimensional cylinder radius. The obtained high-order approximation accurately simulates the physical effects of the transient regime, when the cylinder is set into motion in a two-layer fluid. Our results establish that the role of non-linearity and gravitational forces in determining the interfacial wave field is less significant in a two-layered fluid than in a single-layer fluid. In the limit of a small density difference, the amplitude of the interfacial wave generated by a cylinder moving in the lower layer is half the amplitude of the free surface wave produced by the same cylinder motion in a homogeneous fluid. Furthermore, the unsteady hydrodynamic forces acting on the cylinder exhibit non-monotonic dynamics, which is induced by forced oscillations of the interface.

Understanding the basic principles governing the early-stage formation of waves in a two-layered fluid, due to a submerged body moving near the interface, is crucial for the safe operation of underwater submarines and efficient wave energy absorption of submerged wave-energy devices.

**Funding.** Support from XJTLU Research Development Fund RDF-23-0-031 (first author) is gratefully acknowledged.

**Declaration of interests.** The authors report no conflict of interest.

## Appendix A. Expansions of functions and integral operators

This section provides the explicit expressions for the terms used in the asymptotic solution, including those for the interface displacement and the fluid velocity componenents on it.

The functions $\phi_n(x)$, $\varphi_n(x)$ and $\psi_n(x)$, as defined by (4.7), (4.23) and (4.24), for $n = 1, 3$ admit the following explicit representations:

$$\phi_1(x) = 0, \quad \phi_3(x) = \frac{1}{6}\left(-u_1^2(x) + \rho w_1^2(x) + (1-\rho)(v_1^2(x) - \lambda v_1(x))\right)', \tag{A1}$$

$$\varphi_1(x) = v_1^d(x), \quad \varphi_3(x) = v_3^d(x) + r^2 B_2^r v_1(x) - A_2 v_1(x) - r^2 A_2^r v_1(x), \tag{A2}$$

$$\psi_1(x) = 0, \quad \psi_3(x) = A_2 v_1(x). \tag{A3}$$

For mathematical consistency, we introduce the auxiliary functions

$$\chi_1(x) = r^2(B_0^r u_1(x) - A_0^r v_1(x)), \quad \chi_3(x) = r^2(B_0^r u_3(x) - A_0^r v_3(x)), \tag{A4}$$



https://doi.org/10.1017/jfm.2026.11884 Published online by Cambridge University Press

which aggregate the terms proportional to $r^2$ in the integral equations (4.21).

This paper considers motion with constant acceleration from rest with zero initial speed. Consequently, the functions $\phi_n$, $\varphi_n$, $\psi_n$ and $\chi_n$ with even-numbered indices must vanish. Furthermore, since the quantities in the system of equations (4.5), (4.6), (4.21) and (4.22) depend on the square of radius $r$, these functions can be further expanded in even powers of $r$ as

$$f_n = f_{n,2}r^2 + f_{n,4}r^4 + \cdots, \tag{A5}$$

where $f_n$ can represent the functions $\phi_n(x)$, $\varphi_n(x)$, $\psi_n(x)$, $\chi_n(x)$, $v_n^d(x)$ or the coefficients in the temporal expansions of the integral operators $A_n$, $B_n$, $A_n^r$ or $B_n^r$. Proceeding with this expansion for the coefficients in (A1)–(A4) as power series $r$ yields the following expressions:

$$\phi_{1,2}(x) = 0, \quad \phi_{1,4}(x) = 0, \quad \phi_{3,2}(x) = -\frac{\lambda}{6}(1-\rho)v'_{1,2}(x), \tag{A6}$$

$$\phi_{3,4}(x) = -\frac{1}{6}\left(u_{1,2}(x)^2 - \rho w_{1,2}(x)^2 - (1-\rho)v_{1,2}^2(x)\right)' - \frac{\lambda}{6}(1-\rho)v'_{1,4}(x), \tag{A7}$$

$$\varphi_{1,2}(x) = v_{1,2}^d(x), \quad \varphi_{1,4}(x) = 0, \quad \varphi_{3,2}(x) = v_{3,2}^d(x), \tag{A8}$$

$$\varphi_{3,4}(x) = v_{3,4}^d(x) + B_{2,0}^r u_{1,2}(x) - A_{2,2}v_{1,2}(x) - A_{2,0}^r v_{1,2}(x). \tag{A9}$$

$$\psi_{1,2}(x) = 0, \quad \psi_{1,4}(x) = 0, \quad \psi_{3,2} = 0, \quad \psi_{3,4} = A_{2,2}v_{1,2}, \tag{A10}$$

$$\chi_{1,2}(x) = 0, \quad \chi_{1,4}(x) = (B_{0,0}^r u_{1,2} - A_{0,0}^r v_{1,2}), \tag{A11}$$

$$\chi_{3,2}(x) = 0, \quad \chi_{3,4}(x) = (B_{0,0}^r u_{3,2} - A_{0,0}^r v_{3,2}). \tag{A12}$$

The dipole terms are expressed in terms of the kernel functions $p(x)$ and $q(x)$:

$$v_{1,2}^d(x) = 4(q'(x)\sin\theta - p'(x)\cos\theta), \tag{A13}$$

$$v_{3,2}^d(x) = 4(p''(x)\cos 2\theta - q''(x)\sin 2\theta), \tag{A14}$$

$$v_{3,4}^d(x) = \frac{2}{3}(1+a)\left(p^{(4)}(x)\cos 2\theta - q^{(4)}(x)\sin 2\theta\right). \tag{A15}$$

The leading-order terms in the expansions (4.12) and (4.13) for the integral operators are given by the following expressions:

$$A_{0,0}^r v(x) = \frac{q'(x)}{\pi}\int_{-\infty}^{\infty} p(s)v(s)\,\mathrm{d}s - \frac{p'(x)}{\pi}\int_{-\infty}^{\infty} q(s)v(s)\mathrm{d}s, \tag{A16}$$

$$B_{0,0}^r u(x) = \frac{q'(x)}{\pi}\int_{-\infty}^{\infty} q(s)u(s)\,\mathrm{d}s + \frac{p'(x)}{\pi}\int_{-\infty}^{\infty} p(s)u(s)\,\mathrm{d}s, \tag{A17}$$

$$A_{2,0}^r v(x) = \frac{q'(x)}{\pi}\int_{-\infty}^{\infty} P_{2,0}(s)v(s)\,\mathrm{d}s - \frac{p'(x)}{\pi}\int_{-\infty}^{\infty} Q_{2,0}(s)v(s)\,\mathrm{d}s \tag{A18}$$

$$+ \frac{Q'_{2,0}(x)}{\pi}\int_{-\infty}^{\infty} p(s)v(s)\mathrm{d}s - \frac{P'_{2,0}(x)}{\pi}\int_{-\infty}^{\infty} q(s)v(s)\mathrm{d}s, \tag{A19}$$

$$B_{2,0}^r u(x) = \frac{q'(x)}{\pi}\int_{-\infty}^{\infty} Q_{2,0}(s)u(s)\,\mathrm{d}s + \frac{p'(x)}{\pi}\int_{-\infty}^{\infty} P_{2,0}(s)u(s)\,\mathrm{d}s \tag{A20}$$



https://doi.org/10.1017/jfm.2026.11884 Published online by Cambridge University Press

$$+\frac{Q'_{2,0}(x)}{\pi}\int_{-\infty}^{\infty} q(s)v(s)\,\mathrm{d}s+\frac{P'_{2,0}(x)}{\pi}\int_{-\infty}^{\infty} p(s)v(s)\mathrm{d}s, \tag{A21}$$

$$A_{2,2}v(x)=\frac{1}{\pi}\int_{-\infty}^{\infty}\frac{\eta_{2,2}(x)-\eta_{2,2}(s)}{(x-s)^2}v(s)\,\mathrm{d}s-\frac{\eta'_{2,2}(x)}{\pi}\int_{-\infty}^{\infty}\frac{v(s)\,\mathrm{d}s}{x-s}. \tag{A22}$$

Here,

$$P_{2,0}(x)=q'(x)\sin\theta-p'(x)\cos\theta,\quad Q_{2,0}(x)=-q'(x)\cos\theta-p'(x)\sin\theta \tag{A23}$$

are the leading order terms in the asymptotic expansion of the kernels $P(x)$ and $Q(x)$ with respect to time and radius.

The calculation of the coefficients in the asymptotic expansion of the solution, detailed in Appendix B, requires evaluating the action of integral operators (A16)–(A22) on the functions (A13)–(A15):

$$\begin{aligned}
A^r_{0,0}v^d_{1,2}(x)&=q'(x)\sin\theta-p'(x)\cos\theta,\quad & B^r_{0,0}v^d_{1,2}(x)&=q'(x)\cos\theta+p'(x)\sin\theta,\\
A^r_{0,0}\big(v^d_{1,2}\big)'(x)&=q'(x)\cos\theta+p'(x)\sin\theta,\quad & B^r_{0,0}\big(v^d_{1,2}\big)'(x)&=-q'(x)\sin\theta+p'(x)\cos\theta,\\
A^r_{0,0}v^d_{3,2}(x)&=-q'(x)\cos2\theta-p'(x)\sin2\theta,\quad & B^r_{0,0}v^d_{3,2}(x)&=q'(x)\sin2\theta-p'(x)\cos2\theta,\\
A^r_{2,0}v^d_{1,2}(x)&=p''(x)\cos2\theta-q''(x)\sin2\theta,\quad & B^r_{2,0}v^d_{1,2}(x)&=p'(x)-p''(x)\sin2\theta\\
& & &\quad -q''(x)\cos2\theta.
\end{aligned} \tag{A24}$$

Using the fact that the first term in the expression for the integral operator $A_2$ (4.14) can be represented as the commutator of the Hilbert transform $H$ with the spatial derivative $d/\mathrm{d}x$, we obtain

$$\begin{aligned}
A_{2,2}v^d_{1,2}(x)&=\frac{1+a}{4}H\frac{\mathrm{d}}{\mathrm{d}x}\left(v^d_{1,2}(x)\right)^2-\frac{1+a}{4}\frac{\mathrm{d}}{\mathrm{d}x}\left(v^d_{1,2}(x)Hv^d_{1,2}(x)\right)\\
&=(1+a)(q'(x)-p''(x))
\end{aligned} \tag{A25}$$

In our derivations, we extensively use the fundamental property that any product of the functions $p(x)$, $q(x)$ and their derivatives can be transformed into a linear combination of these functions. This simplification is possible due to the algebraic properties of the underlying rational functions, as captured by the following identities:

$$p'^2(x)=\frac{1}{4}p(x)+\frac{1}{4}q'(x)+\frac{1}{12}q'''(x),\quad q'^2(x)=\frac{1}{4}p(x)+\frac{1}{4}q'(x)-\frac{1}{12}q'''(x), \tag{A26}$$

$$p'(x)q'(x)=-\frac{1}{12}p'''(x),\quad \cdots. \tag{A27}$$

Consequently, the nonlinear terms appearing in the above-mentioned formulae can be reduced to the following linear combinations:

$$(v^d_{1,2}(x))^2=4p(x)+4q(x)'+\frac{4}{3}\big(p'''(x)\sin2\theta+q'''(x)\cos2\theta\big), \tag{A28}$$

$$(Hv^d_{1,2}(x))^2=4p(x)+4q(x)'-\frac{4}{3}\big(p'''(x)\sin2\theta+q'''(x)\cos2\theta\big), \tag{A29}$$

$$v^d_{1,2}(x)Hv^d_{1,2}(x)=-\frac{4}{3}p'''(x)\cos2\theta+\frac{4}{3}q'''(x)\sin2\theta. \tag{A30}$$



https://doi.org/10.1017/jfm.2026.11884 Published online by Cambridge University Press

## Appendix B. Derivation of the asymptotic solution

In this section, we provide the details of the derivation of the asymptotic solution. Collecting terms of equal order with respect to parameter $r$ in expansions of (4.5), (4.6), (4.21) and (4.22), we obtain the system of equations with Hilbert transform:

$$\eta_{n+1,k} = v_{n,k}/(n+1), \tag{B1}$$

$$u_{n,k} - \rho w_{n,k} = \phi_{n,k}, \tag{B2}$$

$$v_{n,k} - H u_{n,k} = \varphi_{n,k} + \chi_{n,k}, \tag{B3}$$

$$v_{n,k} + H w_{n,k} = \psi_{n,k}. \tag{B4}$$

In this section, the dependence of the functions on coordinate $x$ and time $t$ is omitted for clarity of mathematical expressions.

For each integer $n = 1, 2, \ldots$ and even integer $k = 2, 4, \ldots$, the system (B2)–(B4) can be solved recursively for the coefficients $u_{n,k}$, $w_{n,k}$ and $v_{n,k}$, as the right-hand side terms depend on coefficients from the previous order in parameter $r$. Furthermore, using the property that the Hilbert transform is self-inverse ($H^{-1} = -H$), we obtain

$$u_{n,k} = \frac{1+a}{2}\phi_{n,k} + \frac{1-a}{2} H\left(\varphi_{n,k} - \psi_{n,k} + \chi_{n,k}\right), \tag{B5}$$

$$w_{n,k} = -\frac{1+a}{2}\phi_{n,k} + \frac{1+a}{2} H\left(\varphi_{n,k} - \psi_{n,k} + \chi_{n,k}\right), \tag{B6}$$

$$v_{n,k} = \frac{1-a}{2}\psi_{n,k} + \frac{1+a}{2}\left(\varphi_{n,k} + H\phi_{n,k} + \chi_{n,k}\right). \tag{B7}$$

The expressions of the leading-order coefficients for $\phi_{n,k}$, $\varphi_{n,k}$, $\psi_{n,k}$ and $\chi_{n,k}$ are provided in Appendix A.

The recursive procedure starts with the calculation of the first-order solution from (B5)–(B7) for $n = 1$ and $k = 2$:

$$u_{1,2} = \frac{1-a}{2} H v^d_{1,2}, \quad w_{1,2} = \frac{1+a}{2} H v^d_{1,2}, \quad v_{1,2} = \frac{1+a}{2} v^d_{1,2}, \tag{B8}$$

where the function $v^d_{1,2}$ is given by (A13).

Inserting the coefficients from (B8) into system (B5)–(B7) for $n = 1$ and $k = 4$, and solving the resulting equations, we obtain the next-order coefficients in the expansion with respect to the radius $r$:

$$u_{1,4} = -\frac{(1-a^2)}{4}\left(\rho B^r_{0,0} + H A^r_{0,0}\right) v^d_{1,2}, \tag{B9}$$

$$w_{1,4} = -\frac{(1+a)^2}{4}\left(\rho B^r_{0,0} + H A^r_{0,0}\right) v^d_{1,2}, \tag{B10}$$

$$v_{1,4} = \frac{(1+a)^2}{4}\left(\rho H B^r_{0,0} - A^r_{0,0}\right) v^d_{1,2}. \tag{B11}$$

Details of the action of the integral operators appearing in (B9)–(B11) are provided in Appendix A.

Having determined the leading-order terms, we proceed to the next order in the time expansion following the same derivation procedure, for which the solutions take the form:



https://doi.org/10.1017/jfm.2026.11884 Published online by Cambridge University Press

$$u_{3,2} = \frac{1-a}{2} H v^d_{3,2} - \frac{\lambda a(1+a)}{12} \left(v^d_{1,2}\right)', \tag{B12}$$

$$w_{3,2} = \frac{1+a}{2} H v^d_{3,2} + \frac{\lambda a(1+a)}{12} \left(v^d_{1,2}\right)', \tag{B13}$$

$$v_{3,2} = \frac{1+a}{2} v^d_{3,2} - \frac{\lambda a(1+a)}{12} H \left(v^d_{1,2}\right)'. \tag{B14}$$

Here, the prime denotes differentiation with respect to the spatial coordinate. Note that the coefficients $u_2$, $v_2$, $w_2$ vanish, since the right-hand side functions $\phi_2$, $\varphi_2$ and $\psi_2$ are zero at this order. Consequently, the resulting system of integral equations becomes degenerate.

The computation of the coefficient $v_{3,4}$ is substantially more complicated, as it requires the action of several higher-order integral operators discussed in Appendix A. Since the expansion is not carried beyond this order here, only the vertical velocity is required for determining the interface displacement and we therefore restrict the presentation to its calculation:

$$\begin{aligned} v_{3,4} = {} & \frac{1+a}{2} v^d_{3,4} + \frac{1+a}{2} \left( B^r_{0,0} u_{3,2} - A^r_{0,0} v_{3,2} + B^r_{2,0} u_{1,2} - A^r_{2,0} v_{1,2} \right) - \frac{\lambda a}{6} H v'_{1,4} \\ & + \frac{1+a}{12} H \left( -u^2_{1,2} + \rho w^2_{1,2} + \frac{2a}{1+a} v^2_{1,2} \right)' - a A_{2,2} v_{1,2}. \end{aligned} \tag{B15}$$

Substituting the lower-order solutions (B8), (B11), (B12) and (B14) into (B15), we express the higher-order solution in terms of the dipole velocity contributions:

$$\begin{aligned} v_{3,4} = {} & \frac{1+a}{2} v^d_{3,4} + \frac{(1+a)^2}{4} \left( \left( \rho B^r_{0,0} H - A^r_{0,0} \right) v^d_{3,2} + \left( \rho B^r_{2,0} H - A^r_{2,0} \right) v^d_{1,2} \right) \\ & + \frac{a(1+a)^2}{24} H \left( \rho \left( H v^d_{1,2} \right)^2 + \left( v^d_{1,2} \right)^2 \right)' - \frac{a(1+a)}{2} A_{2,2} v^d_{1,2} \\ & + \frac{\lambda a(1+a)^2}{24} \left( \left( \rho B^r_{0,0} v^d_{1,2} + H A^r_{0,0} v^d_{1,2} \right)' + (H A^r_{0,0} - B^r_{0,0}) \left( v^d_{1,2} \right)' \right). \end{aligned} \tag{B16}$$

As a result, the unknown coefficients can be expressed in terms of the functions $v^d_{1,2}$, $v^d_{3,2}$ and $v^d_{3,4}$, which are computed in Appendix A, along with their images under the relevant integral operators. The coefficients $\eta_{2,2}$, $\eta_{2,4}$, $\eta_{4,2}$ and $\eta_{4,4}$ are then obtained by substituting the expressions (B8), (B11), (B14) and (B16), respectively, into relation (B1). The final solutions for $\eta_2$ and $\eta_4$ are given in § 7.

To derive the small-time asymptotic expansion of the hydrodynamic forces acting on a cylinder, we use the asymptotic solution obtained previously to compute the terms in the expansion of the function $F^{(n)}$, defined by (5.7) in § 5:

$$F_{1,2}(z) = \frac{1}{2\pi i} \int_{-\infty}^{+\infty} \frac{i v_{1,2}(x) - u_{1,2}(x)}{x - z} \, \mathrm{d}x = -\frac{2a e^{-i\theta}}{(z-i)^2}, \tag{B17}$$

$$F^{(1)}_{1,2}(z) = \frac{1}{2\pi i} \int_{-\infty}^{+\infty} \frac{i v_{1,2}(x) - u_{1,2}(x)}{(x - z)^2} \, \mathrm{d}x = \frac{4a e^{-i\theta}}{(z-i)^3}, \tag{B18}$$

$$F_{1,4}(z) = \frac{1}{2\pi i} \int_{-\infty}^{+\infty} \frac{i v_{1,4}(x) - u_{1,4}(x)}{x - z} \, \mathrm{d}x = \frac{1}{4} \frac{(5a - 3a^2) e^{-i\theta}}{(z-i)^2}, \tag{B19}$$



https://doi.org/10.1017/jfm.2026.11884 Published online by Cambridge University Press

$$F_{3,2}(z)=\frac{1}{2\pi i}\int\limits_{-\infty}^{+\infty}\frac{iv_{3,2}(x)-u_{3,2}(x)}{x-z}\mathrm{d}x=\frac{-4\left(ae^{-2i\theta}+ia(1+a)\lambda/6e^{-i\theta}\right)}{(z-i)^3},\quad\text{(B20)}$$

$$F_{3,4}(z)=\frac{1}{2\pi i}\int\limits_{-\infty}^{+\infty}\frac{iv_{3,4}(x)-u_{3,4}(x)}{x-z}\,\mathrm{d}x+\frac{1}{2\pi i}\int\limits_{-\infty}^{+\infty}\frac{\eta_{2,2}(v_{1,2}(x)+iu_{1,2}(x))}{(x-z)^2}\,\mathrm{d}x.\quad\text{(B21)}$$

Here, the following property of the kernel functions $p(x)$ and $q(x)$ is used:

$$\frac{1}{\pi}\int\limits_{-\infty}^{+\infty}\frac{p^{(n)}(x)\,\mathrm{d}x}{(x-z)^m}=-\frac{i}{\pi}\int\limits_{-\infty}^{+\infty}\frac{q^{(n)}(x)\,\mathrm{d}x}{(x-z)^m}=\frac{(-1)^{m+n}(n+m-1)!}{(m-1)!(z-i)^{m+n}}\quad(\mathrm{Im}\,z<0),\quad\text{(B22)}$$

($m\geqslant 1$, $n\geqslant 0$ – integers; $p^{(n)}=\partial_x^n\,p$, $q^{(n)}=\partial_x^n\,q$).

The coefficients calculated here are then substituted into the following expansion for the hydrodynamic force from (5.6):

$$\frac{X-iY}{2\pi r^2}=-\frac{1}{2}\overline{z_c''}+F_{1,2}(z_c)r^2+F_{1,4}(z_c)r^4+t^2\left(3F_{3,2}(z_c)r^2+3F_{3,4}(z_c)r^4+\overline{F_{1,2}(z_c)}F_{1,2}^{(1)}(z_c)r^4\right)+O\left(t^4+r^6\right),\quad\text{(B23)}$$

where

$$F_{n,k}^{(m)}=\frac{1}{2\pi i}\int_{-\infty}^{\infty}\frac{iv_{n,k}(x)-u_{n,k}(x)}{(x-z)^{m+1}}\,\mathrm{d}x\quad\text{(B24)}$$

for $m\geqslant 0$, odd integers $n$ and even integers $k$. The explicit expressions for these terms are given in Appendix A. The final asymptotic solution for the hydrodynamic force, obtained by substituting (B17)–(B21) into the expansion (B23), is presented in § 5.

## References


Andrews, L.C. & Shivamoggi, B.K. 1998 *Integral Transforms for Engineers*, p. 353. Macmillian Publishing Company.

Bukreev, V.I., Gusev, A.V. & Sturova, I.V. 1983 Unsteady motion of a circular cylinder in a two-layer liquid. *J. Appl. Mech. Tech. Phys.* **24**, 856–861.

Bukreev, V.I., Gusev, A.V. & Sturova, I.V. 1986 Generation of internal waves under the combined translational and vibrational motion of a cylinder in a fluid bilayer. *J. Appl. Mech. Tech. Phys.* **3**, 375–381.

Dagan, G. & Miloh, T. 1982 Free-surface flow past oscillating singularities at resonant frequency. *J. Fluid Mech.* **120**, 139–154.

Das, D. & Mandal, B.N. 2007 Wave scacttering by a horizontal circular cylinder in a two-layer fluid with an ice-cover. *Intl J. Engng Sci.* **45**, 842–872.

Dean, W.R. 1948 On the reflection of surface waves by a circular cyliinder. *Proc. Camb. Phil. Soc.* **44**, 483–491.

Ekman, V.W. 1904 *On Dead Water in Norwegian North Polar Expedition 1893–1896*, pp. 1–150. Longmans, Green and Co..

Ermanyuk, E.V. & Gavrilov, N.V. 2005 Experimental study on dynamic effect of an internal solitary wave on a submerged circular cylinder. *J. Appl. Mech. Tech. Phys.* **46**, 800–806.

Golikov, A.E. & Makarenko, N.I. 2022 Hydrodynamic loads during acceleration of a cylinder under a free surface. *J. Appl. Mech. Tech. Phys.* **63**, 806–815.

Golikov, A.E. & Makarenko, N.I. 2024 Free motion of a cylinder under the deep fluid surface. *J. Appl. Mech. Tech. Phys.* **65**, 858–865.




https://doi.org/10.1017/jfm.2026.11884 Published online by Cambridge University Press

GORLOV, S.I. 2000 Nonlinear problem of a circular cylinder rising vertically to an interface between liquid media. *J. Appl. Mech. Tech. Phys.* **41**, 280–285.
GREENHOW, M. 1988 Water-entry and -exit of a horizontal circular cylinder. *Appl. Ocean Res.* **10**, 191–198.
GRUE, J., BOURGAULT, D. & GALBRAITH, P.S. 2016 Supercritical dead water: effect of nonlinearity and comparison with observations. *J. Fluid Mech.* **803**, 436–465.
GRUE, J. & PALM, E. 1985 Wave radiation and wave diffraction from a submerged body in a uniform current. *J. Fluid Mech.* **151**, 76–84.
HAUSSLING, H.J. & COLEMAN, R.M. 1979 Nonlinear water waves generated by an accelerated circular cylinder. *J. Fluid Mech.* **461**, 343–364.
HAVELOCK, T.H. 1927 The method of images in some problems of surface waves. *Proc. R. Soc. Lond. A* **115**, 268–280.
HAVELOCK, T.H. 1949 The wave resistance of a cylinder started from rest. *Q. J. Mech. Appl. Maths* **11**, 325–334.
KASSEM, S.E. 1982 Multipole expansions for two superposed fluids, each of finite depth. *Math. Proc. Camb. Phil. Soc.* **91**, 323–329.
KHABAKHPASHEVA, T.I. & STUROVA, I.V. 1998 Diffraction of internal waves by a submerged circular cylinder at forward speed in a two-layer fluid. *J. Engng Maths* **34**, 249–275.
KIM, J.-B., MIN, E.-H. & KOO, W. 2025 Experimental and numerical investigation of the free surface and internal wave characteristics induced by the movement of a 2D cylindrical submerged body in a stratified two-layer fluid. *Ocean Engng* **317**, 120108.
KOSTIKOV, V.K. & MAKARENKO, N.I. 2018 Unsteady free surface flow above a moving circular cylinder. *J. Engng Maths* **112**, 1–16.
LINTON, C.M. & MCIVER, M. 1995 The interaction of waves with horizontal cylinders in two-layer fluids. *J. Fluid Mech.* **304**, 213–229.
MAKARENKO, N.I. 2003 Nonlinear interaction of submerged cylinder with free surface. *J. Offshore Mech. Arctic Engng* **125**, 72–75.
MILOH, T., TULIN, M.P. & ZILMAN, G. 1993 Dead-water effects of a ship moving in stratified seas. *J. Offshore Mech. Arctic Engng* **115**, 105–110.
MOTYGIN, O. & KUZNETSOV, N. 1997 The wave resistance of a two-dimensional body moving forward in a two-layer fluid. *J. Engng Maths* **32**, 53–72.
MOTYGIN, O. & KUZNETSOV, N. 2011 On the forward motion of an interface-crossing body in a two-layer fluid: the role of asymptotics in the problem's statement. *J. Engng Maths* **69**, 113–134.
MOYO, S. & GREENHOW, M. 2000 Free motion of a cylinder moving below and through a free-surface. *Appl. Ocean Res.* **22**, 31–34.
NANSEN, F. 1897 *Farthest North*, vol. 1. Archibald Constalbe.
NORKIN, M.V. 2012 Formation of a cavity in the initial stage of motion of a circular cylinder in a fluid with a constant acceleration. *J. Appl. Mech. Tech. Phys.* **53**, 532–539.
OGILVIE, F. 1963 First- and second-order forces on a cylinder submerged under a free surface. *J. Fluid Mech.* **16** (3), 451–472.
OVSYANNIKOV, L.V., MAKARENKO, N.I., NALIMOV, V.I., LIAPIDEVSKII, V.Y., PLOTNIKOV, P.I., STUROVA, I.V., BUKREEV, V.I. & VLADIMIROV, V.A. 1985 *Nonlinear Problems of the Theory of Surface and Internal Waves*. Nauka.
PARAU, E.I., VANDEN-BROECK, J.-M. & COOKER, M.J. 2007 Nonlinear three-dimensional interfacial flows with a free surface. *J. Fluid Mech.* **591**, 481–494.
PARDO, R.M., BARUA, N., LISAK, D. & NEDIC, J. 2022 Jetting onset on a liquid surface accelerated past a submerged cylinder. *Flow* **2**, E36.
PARDO, R.M. & NEDIC, J. 2021 Free-surface disturbances due to the submersion of a cylindrical obstacle. *J. Fluid Mech.* **926**, A1.
PIERSON, J.-L. & MAGNAUDET, J. 2018*a* Inertial settling of a sphere through an interface. Part 1. From sphere flotation to wake fragmentation. *J. Fluid Mech.* **835**, 762–807.
PIERSON, J.-L. & MAGNAUDET, J. 2018*b* Inertial settling of a sphere through an interface. Part 2. Sphere and tail dynamics. *J. Fluid Mech.* **835**, 808–851.
RAYLEIGH, L. 1882 Investigation of the character of the equilibrium of an incompressible heavy liquid of variable density. *Proc. Lond. Math. Soc.* **14**, 170–177.
SEDOV, L.I. 1965 *Two-Dimensional Problems in Hydrodynamics and Aerodynamics*, p. 427. Interscience Publishers, John Wiley & Sons, Inc.
SEMENOV, Y.A., SAVCHENKO, Y.N. & SAVCHENKO, G.Y. 2021 Impulsive impact of submerged body. *J. Fluid Mech.* **919**, R4.

https://doi.org/10.1017/jfm.2026.11884 Published online by Cambridge University Press

SEONG, W.-J., KOO, W. & MIN, E.-H. 2024 Investigating surface and internal waves and viscosity effects in two-layer fluids with a streamlined moving body using fully nonlinear simulation and experiment. *Ocean Engng* **312**, 119315.

SRETENSKY, L.N. 1937 A theoretical study of wave resistance. *Joukovsky Central Inst. Rep.* **319**, 1–55.

STEPANYANTS, Y.A. & STUROVA, I.V. 2021 Waves on a compressed floating ice plate caused by motion of a dipole in water. *J. Fluid Mech.* **907**, A7.

STOKES, G.G. 1847 On the theory of oscillatory waves. *Trans. Camb. Phil. Soc.* **8**, 314–326.

TELSTE, J.T. 1987 Inviscid flow about a cylinder rising to a free surface. *J. Fluid Mech.* **182**, 149–168.

TRIKOMI, F.G. 1957 *Integral Equations*, p. 238. Interscience.

TUCK, E.O. 1965 The effect of non-linearity at the free surface on flow past a submerged cylinder. *J. Fluid Mech.* **22**, 401–414.

TYVAND, P.A. & KOSTIKOV, V.K. 2023 Impulsive acceleration of a circular cylinder under free surface. *J. Fluid Mech.* **969**, A12.

TYVAND, P.A. & MILOH, T. 1995 Free surface flow due to impulsive motion of a submerged circular cylinder. *J. Fluid Mech.* **286**, 67–101.

URSELL, F. 1950 Surface waves on deep water in the presence of a submerged circular cylinder. I. *Proc. Camb. Phil. Soc.* **46**, 141–152.

VINCENT, L., RIVERO-RODRIGUEZ, J., FALLA, R., ASHRAF, I., TERRAPON, V.E., DORBOLO, S. & SCHEID, B. 2026 Inertial exit dynamics of a horizontal cylinder out of a liquid bath. *J. Fluid Mech.* **1029**, 1–39.

https://doi.org/10.1017/jfm.2026.11884 Published online by Cambridge University Press